
Retrospective Theses and Dissertations

1982

A Calorimeter for Solar Collector Testing Facilities

James C. Huggins
University of Central Florida

 Part of the [Engineering Commons](#)

Find similar works at: <https://stars.library.ucf.edu/rtd>

University of Central Florida Libraries <http://library.ucf.edu>

This Masters Thesis (Open Access) is brought to you for free and open access by STARS. It has been accepted for inclusion in Retrospective Theses and Dissertations by an authorized administrator of STARS. For more information, please contact STARS@ucf.edu.

STARS Citation

Huggins, James C., "A Calorimeter for Solar Collector Testing Facilities" (1982). *Retrospective Theses and Dissertations*. 636.

<https://stars.library.ucf.edu/rtd/636>

A CALORIMETER FOR SOLAR COLLECTOR
TESTING FACILITIES

BY
JAMES CLIFFORD HUGGINS

B.S., University of Texas at Arlington, 1976

RESEARCH REPORT

Submitted in partial fulfillment of the requirements
for the Master of Science in Engineering degree
in the Graduate Studies Program of the College of Engineering
University of Central Florida
Orlando, Florida

Summer Term
1982

ABSTRACT

The reference heat source (RHS) is an electrical calorimeter used with solar collector test facilities. It can be used to calibrate the test facility or to measure the thermal performance of a collector. The RHS described here was designed to be accurate enough to be used as a standard for verification of test facility calibrations. The core of the unit consists of resistance heaters, platinum resistance thermometers, a thermopile, and flow mixers. This core is surrounded by a thermally driven copper shield to control heat loss. The electrical power input to the core is measured with an electronic power transducer. The output of this transducer as well as the temperature sensors is indicated on digital panel meters. All measurements are made independent of the test facility's data acquisition system. The entire unit is mounted on a 0.5 x 1.5 m cart for portability.

In operation, liquid from the test facility is circulated through the RHS core. The liquid is heated by passing over the resistance heaters. If the test facility's calibrations are under investigation, the RHS input power and temperatures are compared with those recorded by the test facility. If a collector is under test, the RHS is placed in series with the collector. The power input to the RHS core heaters is adjusted to give a temperature rise through the RHS equal to some fraction (usually one-half to one) of the temperature rise across the collector. Since the same

mass flow passes through both the RHS and the collector, the energy gain in the collector is simply the RHS input power multiplied by the ratio of the temperature rises.

This RHS was designed for use at temperatures from 0°C to 100°C and liquid flow rates from one to forty liters per minute. The results presented here were obtained using typical flat plate solar collectors. The operational experience obtained in an active test facility is discussed with regard to the achieved accuracy, practical operation, and recommendations for further applications.

ACKNOWLEDGMENTS

I would like to express my sincere thanks to all those who have helped with and contributed to this project. My thanks to Dr. Eno for his assistance with my entire graduate program and his patience in the completion of this work. My thanks to Dr. Bishop and Dr. Chang for their assistance in bringing the report to its final form. I am indebted to John Jenkins of the National Bureau of Standards for his assistance and encouragement early in the project.

The remainder of my thanks go to the marvelous people at the Florida Solar Energy Center without whose assistance and support this work would not have been possible. Funding for the entire project came from the Center's budget and the final product will be used at FSEC in ongoing research projects. To James Roland my thanks for his unending patience and understanding of the problems I have encountered. Yayi Rickling's assistance with the literature search got me off to a good start. I owe a great deal to Craig Maytrott, for without his assistance with the electronics, I would still be struggling along with numerous unsolved problems. My thanks to Leroy Nash for his mechanical design assistance. Construction of the mechanical components was expertly handled by Lew Patton and Joe Hiabach. Much of the electrical construction was

done by Jay Buckholt, Dick Vabrinskas, and Tony LaCourt. My thanks to Michael Beattie for his assistance with the tedious calibration work and to Dennis Crocker for his skillful production of the figures presented here. For typing all of this in a presentable form and being patient through many revisions, I thank Cynthia Abrams.

Finally, I would like to thank my parents for their support, encouragement, concern, assistance, and love over the years. Without them I never would have made it.

TABLE OF CONTENTS

LIST OF FIGURES	vi
LIST OF SYMBOLS	vii
INTRODUCTION	1
I. Theory	5
II. Apparatus.	12
III. Uncertainty Analysis	23
IV. Calibration.	27
V. Operation.	40
Test Facility Verification.	40
Solar Collector Testing	44
VI. Conclusions.	46
References	48
Appendices	50
1. Instrumentation Specifications.	51
2. Calibration Standards Specifications.	53
3. Calibration Data.	55
4. Test Facility Verification Data	62

LIST OF FIGURES

1. Test Facility Verification	6
2. Solar Collector Testing.	9
3. Core Schematic	13
4. Core/Shield Assembly	15
5. Shield Flow Schematic.	17
6. Shield Control Sequence.	19
7. Shield Control Electronics Schematic	20
8. Complete RHS Assembly.	22
9. Operational Calibration Schematic.	29
10. Heat Loss.	31
11. Time Constant.	33
12. RHS Calibration - Initial.	34
13. RHS Calibration - Final.	38
14. Test Facility Verification - Sample 1.	42
15. Test Facility Verification - Sample 2.	43
16. Heat Loss Data Without Shield.	58
17. Heat Loss Data With Sheild	59
18. Initial Calibration Data	60
19. Final Calibration Data	61
20. Facility Verification Data - Sample 1.	64
21. Facility Verification Data - Sample 2.	65

LIST OF SYMBOLS

A	-	surface area
C_p	-	fluid specific heat
I	-	solar irradiance
k	-	thermal conductivity
m	-	mass flow rate
Q	-	energy flow rate
Q_{RHS}	-	Electrical energy input to the core heaters
r	-	radius
T	-	temperature
t	-	time
ΔT	-	temperature difference
η	-	efficiency

Subscripts:

a	-	ambient air
CAL	-	RHS calibration
COLLECTOR	-	solar collector
core	-	RHS core
FACILITY	-	solar collector test facility
i	-	inlet
m	-	mean

o	-	outlet
RHS	-	reference heat source
shield	-	RHS thermal shield
STD	-	calibration standards

INTRODUCTION

The thermal performance of low and medium temperature (10-100°C) solar collectors is currently determined according to ASHRAE standard 96-1980 [1] or 93-77 [2]. The procedure is based on the first law of thermodynamics with the thermal efficiency being defined by

$$\eta = \frac{\text{collector thermal output}}{\text{solar input}} = \frac{m C_p \Delta T}{I} \quad (1)$$

where:

η = collector efficiency

m = mass flow rate through the collector

C_p = specific heat of the transfer fluid

ΔT = temperature rise across the collector

I = solar irradiance in the plane of the collector.

All of the quantities on the right, except C_p , are measured experimentally over the range of operating temperatures normally encountered by the collector. The specific heat is typically taken from reference tables.

The two most difficult quantities to measure experimentally are the mass flow rate and the solar radiation. A solution to the mass flow measurement problem was investigated here. Only those collectors with a liquid transfer fluid were considered. The typical method of mass measurement starts with a volume measurement

which is converted using table values for density. This results in two potential sources of error. Volume is difficult to measure at varying temperatures and the density of the test fluid may not match the table values. Calorimetric techniques have been used to measure fluid flow rates for many years [3, 4]. Basically this involves measuring the fluid temperature rise due to a measured quantity of energy input to a fluid of known specific heat to determine the mass flow rate. The reference heat source (RHS) concept utilizes this technique to eliminate the need for measuring the mass flow rate of the transfer fluid by measuring the electrical input to a set of resistance heaters and the temperature rise of the fluid passing over the heaters. The standard RHS consists of inlet and outlet temperature sensors, resistance heating elements, and a power transducer.

Previous RHS devices have been developed both in Europe and the United States [5-10]. Initially, this concept was applied to the testing of high temperature (300°C+) concentrating collectors where flow measurement is extremely difficult due to the type of fluids used [8]. Later, as the difficulties of flow measurement were further realized, the concept was applied to low and medium temperature collector testing [5-7, 9]. The objective of this study was to develop a reference heat source which could not only be used in the testing of solar collectors, but would also serve to verify the calibration of a test facility's instrumentation.

There are three items which require calibration in a standard RHS. Calibration of the temperature sensors is relatively straight-

forward and well understood. The measurement of electrical power is also possible with reasonable ($\pm 0.5\%$) accuracy. The third item is the rate of heat loss from the RHS. Since some of the energy applied to the heating elements is lost to the surroundings, the ratio of thermal output to electrical input decreases as the operating temperature increases. This heat loss rate must be determined quite accurately so that corrections may be applied to the results obtained. RHS devices constructed at the National Bureau of Standards have used a dewar flask to reduce the heat loss [9]. The European devices have used fiberglass or urethane foam [5, 6]. A high temperature RHS developed at Argonne National Laboratory [8] used an electrical heating tape around the resistance heater assembly to balance the thermal losses. This technique, called thermal shielding, seemed to work well, but had not been applied to low and medium temperature applications until very recently [11].

The technique utilized here involves placing the core assembly in a copper canister to equalize the temperature distribution. This canister is then placed in another copper canister around which copper tubing is wrapped. Water is circulated through this tubing at a carefully controlled temperature. The water temperature is adjusted to keep the temperature difference between the thermal shield canister and the core canister less than one degree Celsius. Since the temperature of the water in the shield is adjustable, heat loss from the core is significantly reduced at all operating temperatures.

Additional improvements suggested by NBS [9] that were incorporated in this RHS include thorough mixing of the fluid before making temperature measurements and the use of cartridge heating elements as opposed to an in-line prepackaged heater unit. Every attempt was made to make this RHS as accurate as possible to enable its use as a calibration reference. It is expected that the RHS concept will soon be used by national certification agencies to accredit solar collector testing laboratories. A much less complex approach has been suggested by Clinton [13], but further comparisons of RHS results are necessary to determine the degree of accuracy required.

CHAPTER I

THEORY

The RHS operates on the basic principle of a calorimeter. The temperature rise of a fluid due to the input of a precisely measured quantity of electric power is used to determine the fluid mass flow rate. The first law of thermodynamics is used to calculate the desired quantity:

$$Q = m C_p \Delta T \quad (2)$$

where

Q = energy flow rate

m = mass flow rate

C_p = fluid specific heat

ΔT = temperature rise of the fluid.

The RHS can be used in two operating modes. In the first mode, it is a calibration standard for determining the accuracy of a solar collector test facility. In this mode the RHS operates as a "black box" while the test facility is used to measure its thermal energy output. Heat transfer fluid is passed through the RHS as if it were a solar collector as shown in Figure 1. Electric power is applied to the RHS core heaters to simulate solar energy input. The test facility measures the fluid temperature rise and flow rate. The data reduction techniques normally employed in

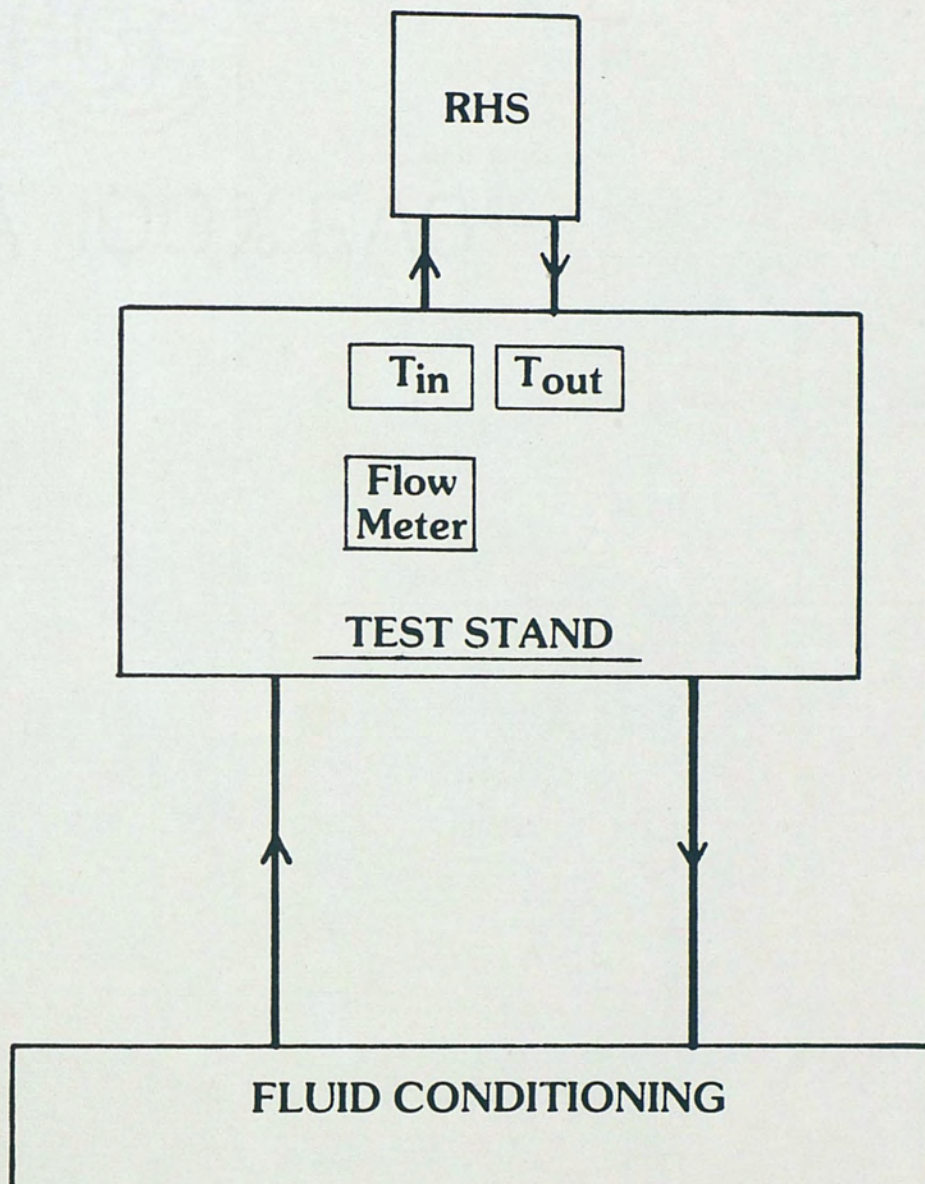


Fig. 1. Test Facility Verification

solar collector testing are used to determine the thermal output of the RHS as if it were a solar collector. Measurements of fluid temperature and volumetric flow rate are combined with table values for the fluid's density and specific heat to arrive at the net energy gain in the fluid.

This energy gain is then compared to the known energy input to the fluid by the RHS. The facility's inlet and outlet temperature sensors are verified by direct comparison. The fluid mass flow rate is compared to the RHS determined flow as calculated from this rearrangement of the first law:

$$m = \frac{Q_{\text{RHS}}}{C_p \Delta T_{\text{RHS}}} \quad (3)$$

where:

Q_{RHS} = electrical energy input to the RHS core heaters

ΔT_{RHS} = temperature rise across the core as measured by the RHS fluid temperature sensors

The net result is verification of both the instrumentation of the facility and the calculation procedures used to determine the energy output of the collector. These tests can be made at all temperatures and flow rates experienced during normal operation. The error analysis of the facility's measurement is presented as recommended by Jenkins and Streed [12]. The percentage error is plotted versus the difference between the average fluid temperature

and the ambient air temperature. The test stand error is defined as the percentage difference between the energy gain determined by the test facility and the directly measured energy input to the RHS:

$$\text{ERROR} = \frac{Q_{\text{FACILITY}} - Q_{\text{RHS}}}{Q_{\text{RHS}}} \quad (4)$$

In the second operating mode, the RHS is used directly to measure the energy output of a solar collector. The collector is mounted as in a normal test as shown in Figure 2. The RHS is placed ahead of and in series with the collector. The transfer fluid from the test facility passes through both the RHS and the collector so that the mass flow rate is the same through each. Combining the first law expressions for the RHS and the collector, the following ratio is obtained:

$$\frac{Q_{\text{RHS}}}{Q_{\text{COLLECTOR}}} = \frac{m C_p \Delta T_{\text{RHS}}}{m C_p \Delta T_{\text{COLLECTOR}}} \quad (5)$$

Since the mass flow rates are the same and the specific heat of the fluid can be considered constant over narrow temperature ranges, this equation reduces to

$$Q_{\text{COLLECTOR}} = Q_{\text{RHS}} \frac{\Delta T_{\text{COLLECTOR}}}{\Delta T_{\text{RHS}}} \quad (6)$$

where the RHS quantities are measured by RHS instrumentation and the collector temperature rise is measured by the test facility's

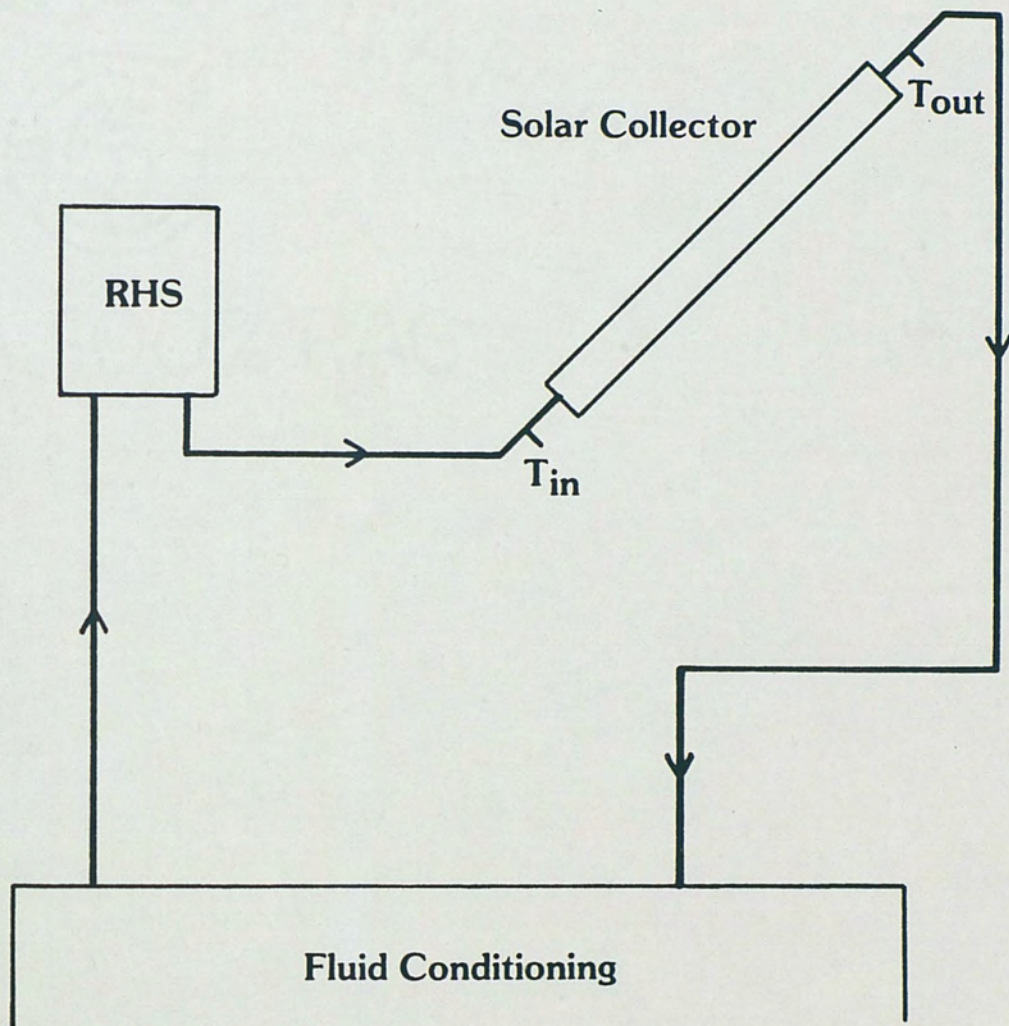


Fig. 2. Solar Collector Testing

instrumentation. If there is a large difference in average fluid temperature between the RHS and the collector, the difference in specific heat can be accounted for as follows:

$$Q_{\text{COLLECTOR}} = Q_{\text{RHS}} \frac{C_{p\text{COLLECTOR}}}{C_{p\text{RHS}}} \frac{\Delta T_{\text{COLLECTOR}}}{\Delta T_{\text{RHS}}} \quad (7)$$

Since the mass flow rate is no longer in these equations, this difficult measurement is eliminated along with the inaccuracy of using tabulated values for fluid density and, in most cases, specific heat.

As energy is added to the fluid by the core heaters, ideally, all of the energy is converted to heat in the fluid and none of it is lost to the surroundings. The deviation from this ideal condition can be measured by proper calibration of the RHS as a complete unit. The magnitude of the deviation is minimized by the use of a thermally driven shield to control heat loss from the core. The temperature of the shield is adjusted to match the temperature of the core such that

$$Q_{\text{loss}} = -k A (T_{\text{core}} - T_{\text{shield}}) / (r_{\text{shield}} - r_{\text{core}}) \cong 0 \quad (8)$$

where

Q_{loss} = heat loss from RHS core

k = combined thermal conductivity of core enclosure, including insulation and shielding canisters

A = Surface area of core enclosure

T_{core} = average temperature of core assembly

T_{shield} = average temperature of thermal shield

r_{shield} = radius of the thermal shield

r_{core} = radius of the core assembly

The actual deviation from ideal operation is discussed further with the presentation of the calibration results in Chapter III.

CHAPTER II

APPARATUS

The RHS consists of two separate fluid systems with electrical supply power and instrumentation for each. The core assembly contains the fluid from the test facility. The thermal shield is a closed loop which controls heat loss from the core.

The core assembly is shown schematically in Figure 3. It is constructed from 2.5 cm copper tubing and fittings. Fluid from the test facility enters from the bottom. It passes through a static flow mixer and follows a right-angle bend before passing over the inlet temperature sensor. The fluid then makes another right-angle bend and passes through the low temperature side of the thermopile. Following a 180° bend, the fluid passes over four 500 watt heating cartridges separated by 180° bends. After a final 180° bend, the fluid passes through a second static flow mixer, around a right-angle bend, and across the outlet temperature sensor. After a final right-angle bend, the fluid passes through the high temperature side of the thermopile and out the bottom to the test facility. Electrical power to the heaters is controlled with four switches. Utility line voltage (120V, 60 Hz) is applied to any combination of heaters, with these switches giving four levels of input power.

Instrumentation in the core consists of two 100 ohm platinum resistance thermometers, a 20-junction type-T thermopile, and a 500

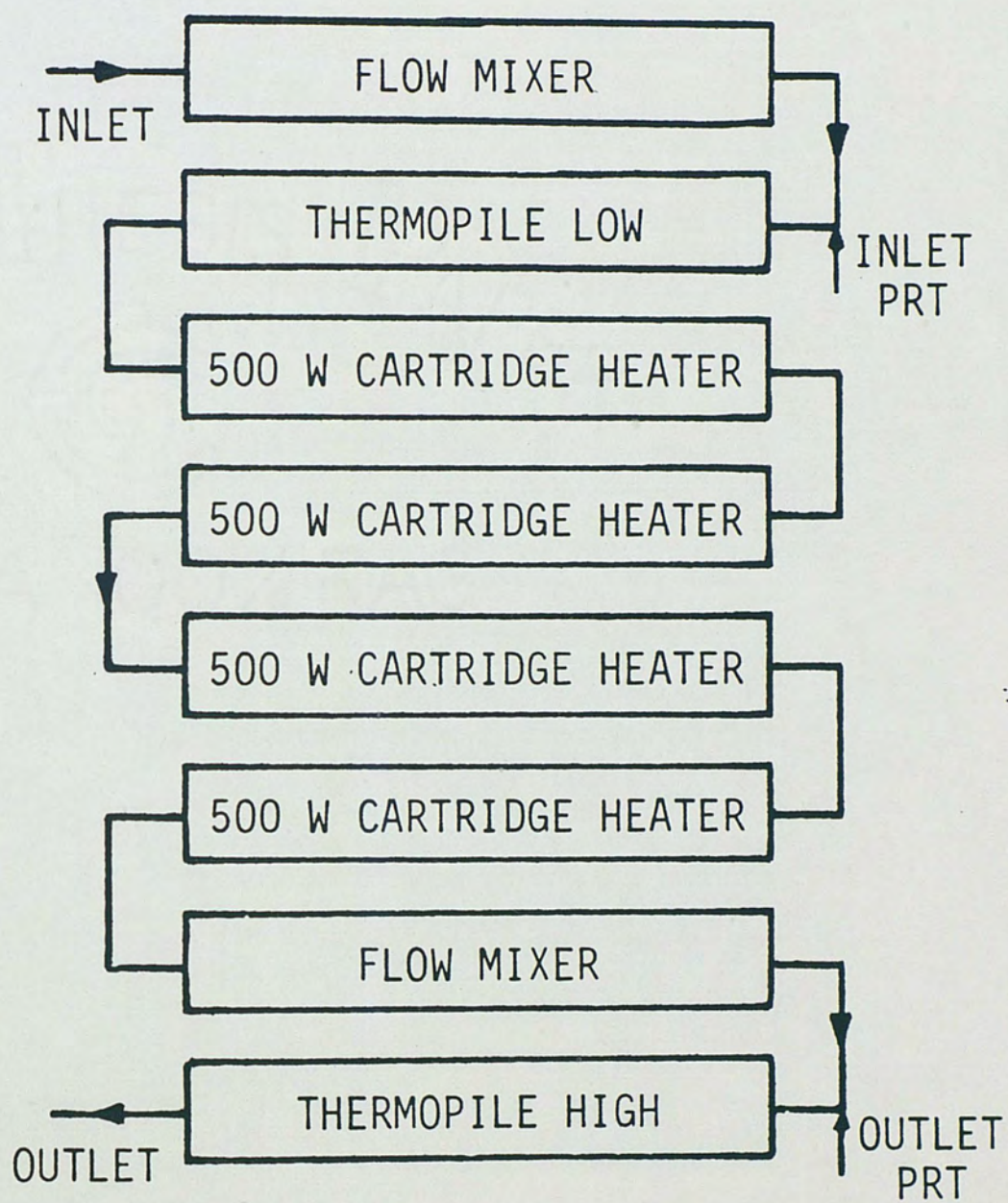


Fig. 3. Core Schematic

watt power transducer. Specifications for this instrumentation are presented in Appendix 1. The platinum resistance thermometers are read with linearizing bridges whose output is displayed on $4\frac{1}{2}$ digit panel meters. The thermopile output is amplified 50 times and displayed on another $4\frac{1}{2}$ digit panel meter. The power transducer is a Hall-effect device which accounts for power factor and has a rated accuracy of 0.5 percent. It produces a one milliamp current output at 500 watts input. Since there are 2,000 watts of heating cartridges in the core, 75 percent of the current is shunted around the power transducer. The transducer output is passed through a 200 ohm precision resistor. The voltage drop across the resistor is displayed on a $4\frac{1}{2}$ digit panel meter resulting in a direct indication of 0-2,000 watts.

The core assembly is housed in three concentric copper canisters with diameters of 30, 35, and 43 cm. The canisters each rest on 2.5 cm of foil-faced polyisocyanurate foam as shown in Figure 4. All air spaces are filled with perlite. A 1.0 cm copper tube is wound in a spiral and soldered to the middle canister. The tubes are approximately three centimeters apart. There are five platinum resistance thermometer elements (encased in ceramic) attached to the outside of the inner canister with thermal cement and five more attached to the outside of the middle canister (between the tubes). Three elements are evenly spaced around the sides of the canisters and one in the center of each end. These elements are connected in series and are used to measure the temperature difference between these two canisters so the water temperature in the shield can be

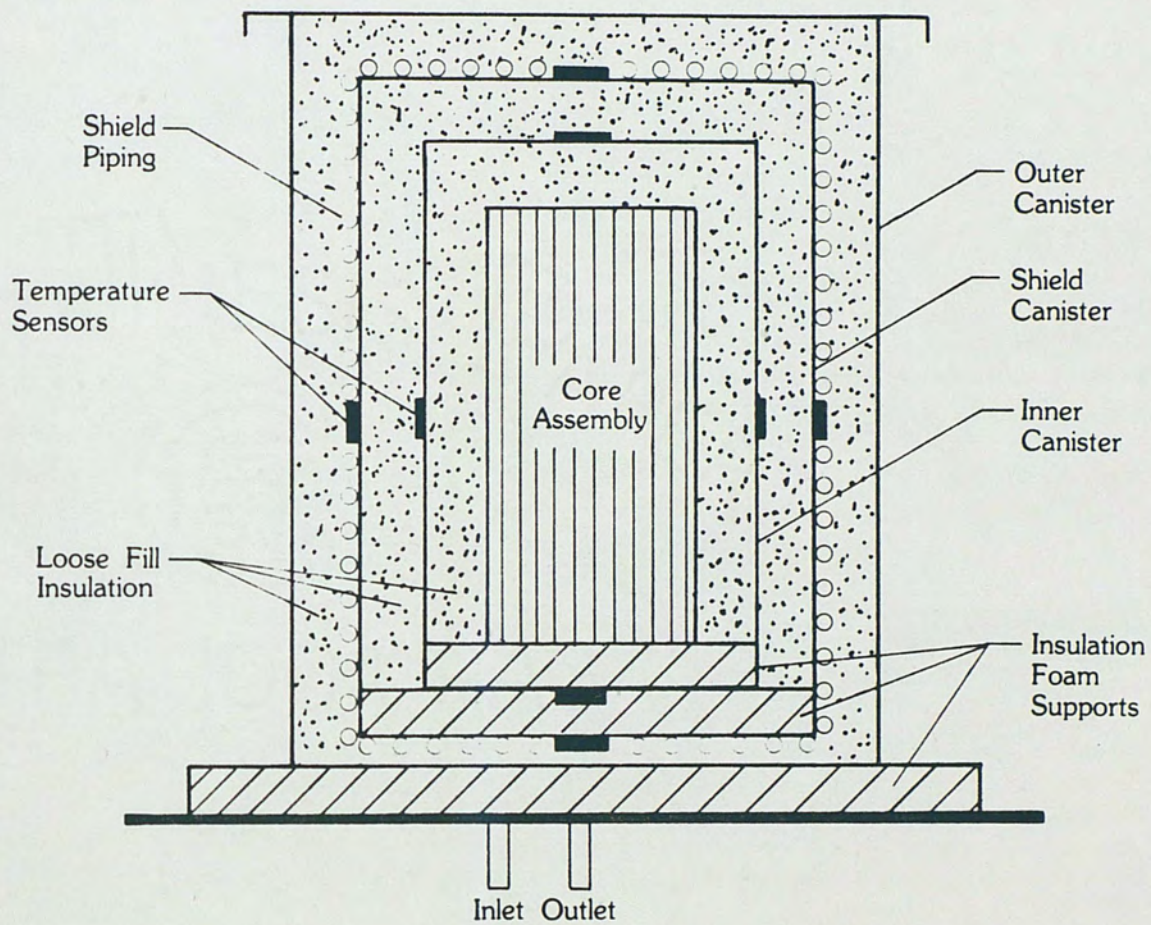


Fig. 4. Core/Shield Assembly

adjusted, if necessary, to bring the canisters to approximately the same temperature. When the inner and middle canisters are the same temperature, the heat loss from the core is, by definition, zero. A $3\frac{1}{2}$ digit panel meter is used to indicate the relative temperatures of the canisters so the operator will know when accurate readings can be made.

The thermal shield loop is shown schematically in Figure 5. It is constructed of 1.0 and 1.3 cm copper tubing. This is a closed loop in which water is recirculated to control heat loss from the core. Starting at the small circulating pump, the water passes through the 1.0 cm copper tubing soldered to the middle copper canister. The water leaves the canisters at the top and passes by an expansion tank made from 6.4 cm copper pipe before reaching valves V1 and V2. These valves control flow through the heat exchanger. The heat exchanger is composed of 2.5 cm wide aluminum fins on copper tubes which make four passes. Two 10 cm diameter muffin fans maintain air flow over the 13 by 37 cm exchanger. The heat exchanger is the first level of cooling and is used when small decreases in core temperature are required. The fans operate only when there is flow through the heat exchanger.

The water next moves to valves V3 and V4. These valves control flow through the ice box. This box is a 30 liter picnic cooler fitted with a coil of 1.0 cm copper tubing. The ice box is filled with ice when it is necessary to operate the RHS below the ambient air temperature. From here the water passes into the heater tank. This tank is made from 6.4 cm copper pipe and con-

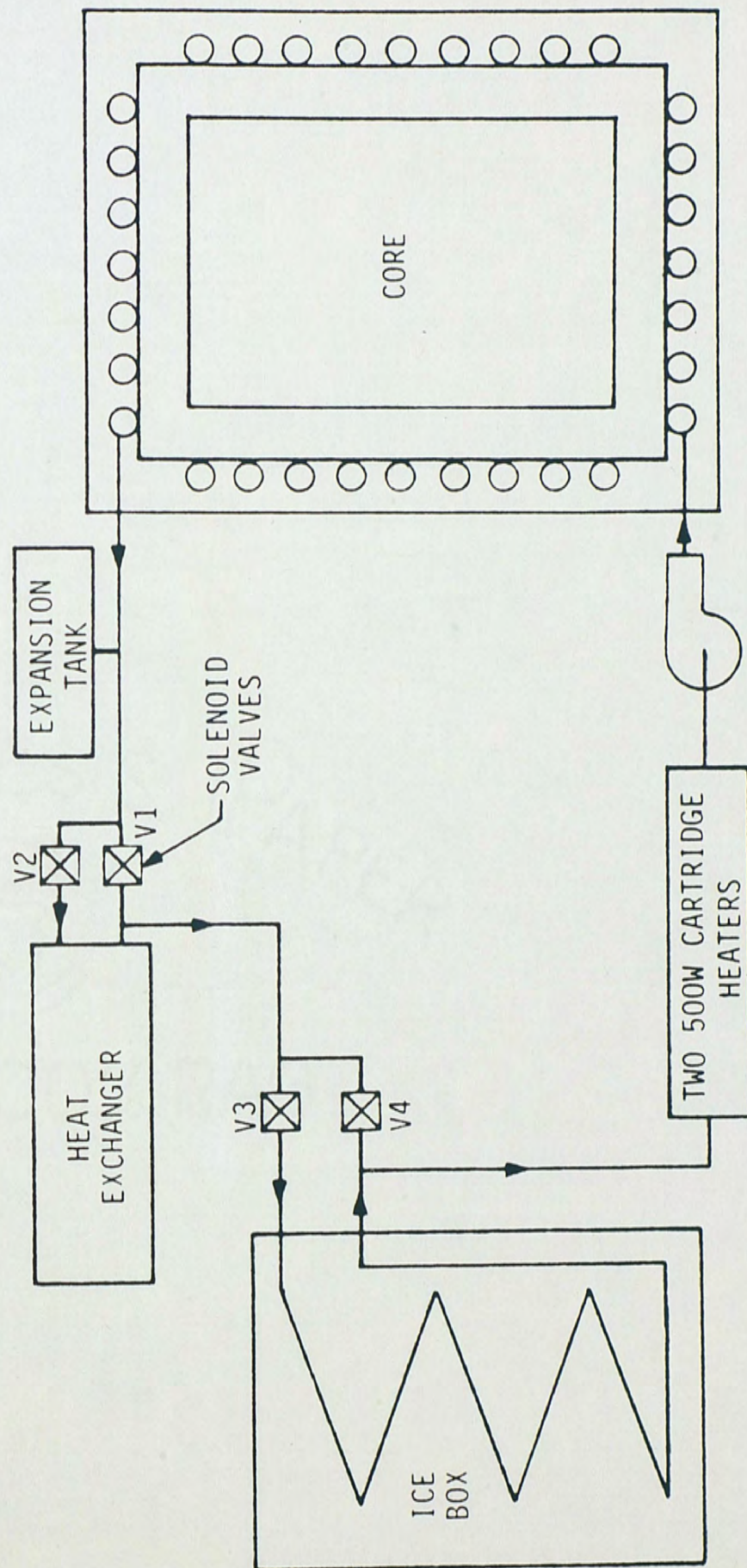


Fig. 5. Shield Flow Schematic

tains two 500-watt heating cartridges. When the core is hotter than the shield, these heaters are activated to raise the shield water temperature. The amount of heat added is proportional to the difference in temperature between the core and the shield. Upon leaving the heater tank the water enters the suction side of the 30-watt circulating pump which operates at all times. Control of the valves, fans, heating elements, and pump in the shield loop is accomplished with electronics designed and built by engineers and technicians at the Florida Solar Energy Center.

The operational sequence of the shield components is shown in Figure 6. When the shield temperature is between one and three degrees Celsius warmer than the core temperature, the heat exchanger valves and fans are activated to reduce the shield water temperature. If the level of cooling is not sufficient, the ice box valves are activated and the heat exchanger is turned off until the shield-core temperature difference is reduced to three degrees Celsius. When the core and shield temperatures are within one degree, the water is simply circulated around the loop, bypassing the heat exchanger and the ice box. When the core temperature exceeds one degree warmer than the shield, the two 500-watt cartridge heaters are activated. The electric input to these heaters is proportionally controlled as a function of the core-shield temperature difference. The power input is controlled from zero at a one degree difference to full power (1000 watts) at a five degree difference. Figure 7 is a simplified schematic of the electrical

	V ₁	V ₂	V ₃	V ₄	FANS	PUMP	HEATERS
S > C	X	0	X	0	0	0	X
S >> C	0	X	0	X	X	0	X
S = C	0	X	X	0	X	0	X
S < C	0	X	X	0	X	0	0

S = shield temperature

C = core temperature

X = off or closed

0 = on or open

Figure 6. Shield Control Sequence

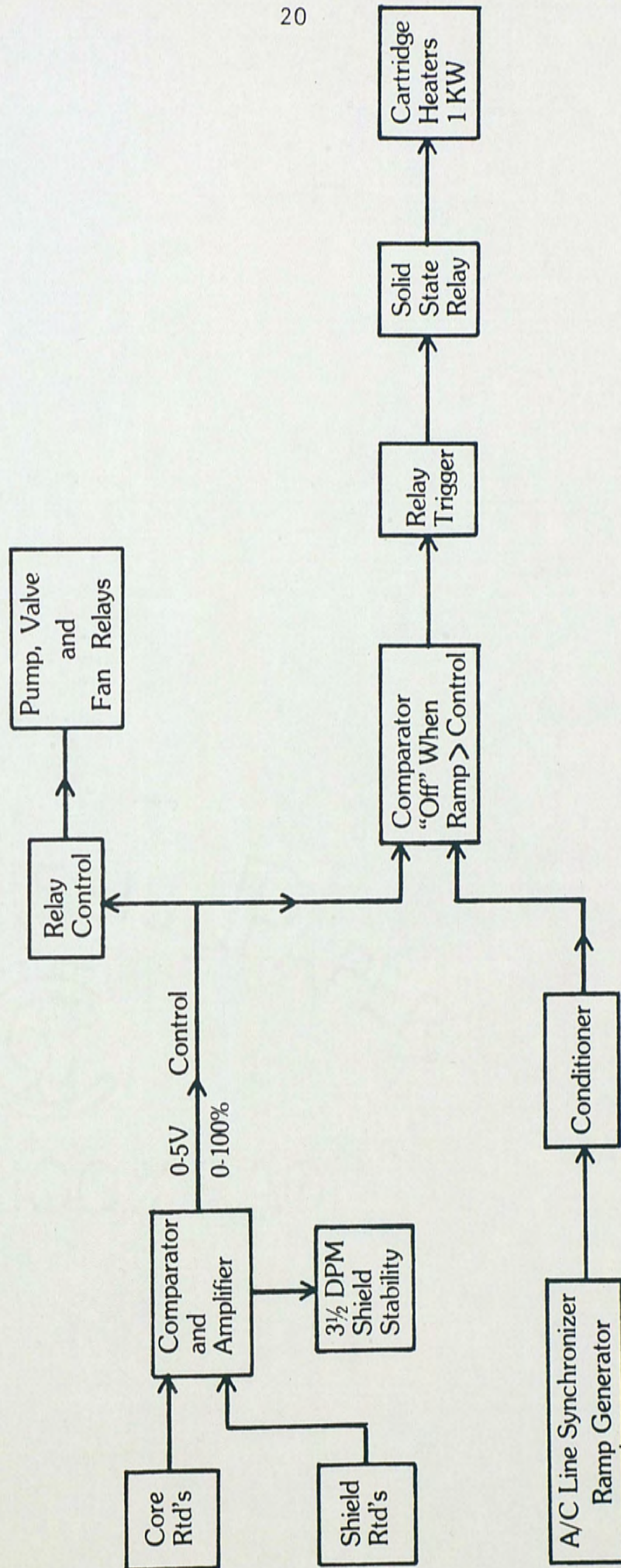


Fig. 7. Shield Control Electronics Schematic

circuit which controls the operation of the shield. Figure 8 presents the complete assembly on its cart.

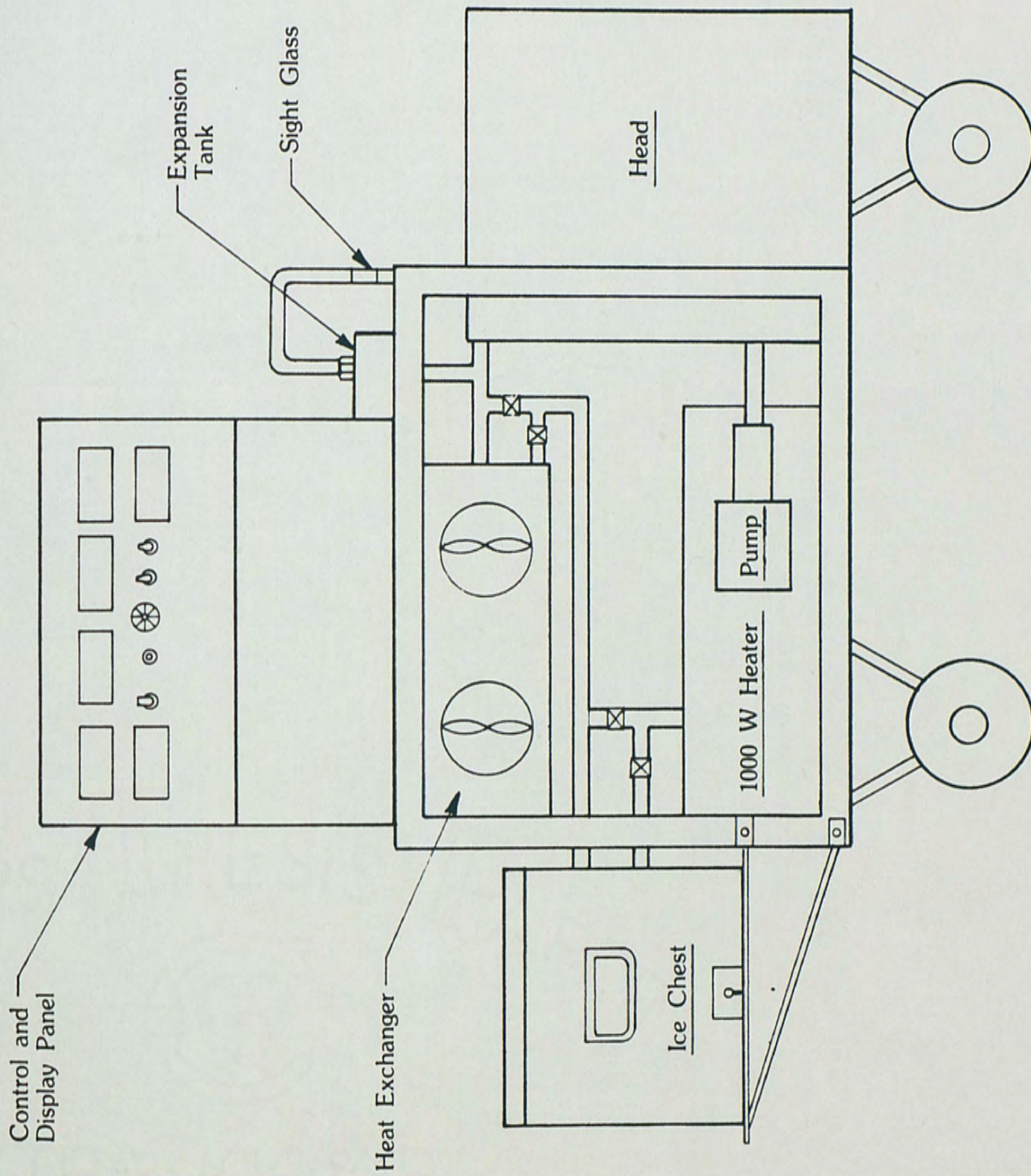


Fig. 8. Complete RHS Assembly

CHAPTER III

UNCERTAINTY ANALYSIS

The efficiency of the RHS is defined as

$$\eta_{\text{RHS}} = \frac{Q_{\text{STD}}}{Q_{\text{RHS}}} = \frac{\frac{m}{t} C_p (T_o - T_i)}{Q_{\text{RHS}}} \quad (9)$$

where

Q_{STD} = heat output of the RHS as measured by the
calibration standards

m = mass of water

t = time during which m is measured

C_p = specific heat of water at average temperature measured
by the calibration standards

T_o = water temperature at outlet of RHS

T_i = water temperature at inlet of RHS

All parameters are maintained as constant as possible during
the time interval over which the mass is measured.

The absolute error introduced by the combination of the errors
in each of the measurements is given by [14]:

$$E_a = \left| \Delta m \frac{\partial \eta_{\text{RHS}}}{\partial m} \right| + \left| \Delta t \frac{\partial \eta_{\text{RHS}}}{\partial t} \right| + \left| \Delta C_p \frac{\partial \eta_{\text{RHS}}}{\partial C_p} \right| + \left| \Delta T_o \frac{\partial \eta_{\text{RHS}}}{\partial T_o} \right| \\ + \left| \Delta T_i \frac{\partial \eta_{\text{RHS}}}{\partial T_i} \right| + \left| \Delta Q_{\text{RHS}} \frac{\partial \eta_{\text{RHS}}}{\partial Q_{\text{RHS}}} \right| \quad (10)$$

which is the result of a Taylor series expansion of the function of
the individual measurements and their absolute errors. The abso-

lute error in each of the individual measurements was selected on the basis of equipment specifications and operational experience to be:

$$\begin{aligned}\Delta m &= \pm 0.11 \text{ Kg} & \Delta T_o &= \Delta T_i = \pm 0.015^\circ\text{C} \\ \Delta t &= \pm 1.0 \text{ sec} & Q_{\text{RHS}} &= \pm 5.0 \text{ watts} \\ C_p &= \pm 4.2 \text{ J/Kg}^\circ\text{C}\end{aligned}$$

These limits are well within the error limits prescribed by the ASHRAE standards.

Complete specifications on all of the calibration equipment are presented in Appendix 2. The absolute error was calculated for each of the RHS calibration points and ranged from $\pm 1.2\%$ at a flow of 0.032 Kg/sec with 1800 watts of input power to $\pm 4.5\%$ at a flow of 0.095 Kg/sec with 500 watts of input power.

An indication of the more probable magnitude of the errors to be expected is given by the root-sum square error:

$$E_{\text{rss}} = \left[\left(\Delta m \frac{\partial \eta_{\text{RHS}}}{\partial m} \right)^2 + \left(\Delta t \frac{\partial \eta_{\text{RHS}}}{\partial t} \right)^2 + \left(\Delta C_p \frac{\partial \eta_{\text{RHS}}}{\partial C_p} \right)^2 + \left(\Delta T_o \frac{\partial \eta_{\text{RHS}}}{\partial T_o} \right)^2 + \left(\Delta T_i \frac{\partial \eta_{\text{RHS}}}{\partial T_i} \right)^2 + \left(\Delta Q_{\text{RHS}} \frac{\partial \eta_{\text{RHS}}}{\partial Q_{\text{RHS}}} \right)^2 \right]^{\frac{1}{2}} \quad (11)$$

which is again based on a Taylor series expansion but which considers the individual errors as statistical bounds rather than absolute limits of error. The root-sum square error was also

calculated for each of the calibration points and ranged from $\pm 0.6\%$ to $\pm 2.1\%$ at the same conditions as the absolute error.

The magnitude of these errors is well within the requirements of the ASHRAE standards [1, 2]. The errors are also consistent with those found by Waksman and Streed [15] in their analysis of data obtained from four solar collector testing laboratories in the United States.

The magnitude of each of the terms in the above two equations indicates the relative significance of the errors in each measurement. It was found that the error due to uncertainty in fluid specific heat was the lowest. This fact, combined with the fact that the specific heat of water changes by only 0.8% from 5°C to 95°C with a maximum change of 0.1% in any 5°C temperature range above 20°C, indicates that the error, when testing solar collectors, due to a temperature difference between the RHS and the collector is negligible unless very large (50°C) temperature differences are encountered. The error due to temperature measurement during calibration was the largest with the mass measurement error being second.

Examination of the possible errors associated with temperature measurement in the RHS revealed the errors indicated as follows:

<u>Component</u>	<u>Nominal Error</u>
Platinum Resistance Thermometer	
o Calibration	$\pm 0.052^{\circ}\text{C}$
o Repeatability	$\pm 0.050^{\circ}\text{C}$
Linearizing Bridge	
o Nominal accuracy	$\pm 0.20^{\circ}\text{C}$
o Ambient Temp. with 10 $^{\circ}\text{C}$ spread	$\pm 0.09^{\circ}\text{C}$
Panel Meter	
o Nominal accuracy	$\pm 0.026^{\circ}\text{C}$
o Temperature stability	<u>$\pm 0.030^{\circ}\text{C}$</u>
	$\pm 0.45^{\circ}\text{C}$

The actual error observed during calibration of the RHS never exceeded $\pm 0.1^{\circ}\text{C}$ however. Calibration of the temperature measurement components as a completely installed system was felt to have improved the overall accuracy.

CHAPTER IV

RHS CALIBRATION

The reference heat source was calibrated against laboratory standards to determine its operating characteristics prior to initiating test facility calibrations or solar collector testing. The digital panel meters were calibrated with a laboratory voltage standard accurate to ± 1 microvolt before attaching the RHS instrumentation. The platinum resistance thermometers were calibrated with their linearizing bridges and the actual connecting cables in place. They were removed from the RHS core unit and placed in an isothermal temperature bath for comparison against mercury in glass thermometers accurate to $\pm 0.01^\circ\text{C}$. The electronic watt transducer was also calibrated as installed in the RHS. A shunt calibrated to $\pm 1.0 \times 10^{-9}$ ohms was placed in series with the heating elements. The voltage drop across this shunt was measured with a differential voltmeter accurate to ± 1 microvolt to determine the current flow. The voltmeter was also used to measure the voltage drop across the heating elements. These measurements of current and voltage were then used to determine the actual power dissipation in the heating elements.

The initial operational calibration was conducted at the glazed collector test facility of the Florida Solar Energy Center using extraordinary care in controlling the fluid flow rate and

temperature. A schematic of the calibration setup is presented in Figure 9.

Operation of the RHS was examined at fluid flow rates of 1.9, 3.8, and 5.7 liters per minute, fluid temperatures of -10, 0, 10, 30, 50, and 70°C above the ambient air temperature and with 0, 500, 1000, 1500, and 2000 watts of input power. The fluid used in all operational calibrations was deionized water.

The mass flow rate was determined using gravimetric methods. A 21.3 liter glass flask was mounted on a beam scale accurate to ± 0.1 kilograms. Flow into the flask was manually controlled in conjunction with a manually operated stop watch accurate to ± 0.1 seconds. Inlet and exit fluid temperatures were measured with mercury in glass thermometers mounted in heavily insulated thermometer wells as illustrated in Figure 9. The wells were constructed of 1.0 and 2.5 cm diameter copper tubing mounted in cardboard boxes insulated with polyisocyanurate foam and perlite. For this initial calibration, the flow of fluid between the core/shield assembly and the thermometer wells was through silicone hoses insulated with high density foam. The hoses were each approximately 75 cm long.

Three graphs were generated to show the overall performance of the RHS. These graphs present the results of the calibration tests in the format recommended by Jenkins and Streed [12] with the exception of error bars which are discussed in the chapter on uncertainty analysis.

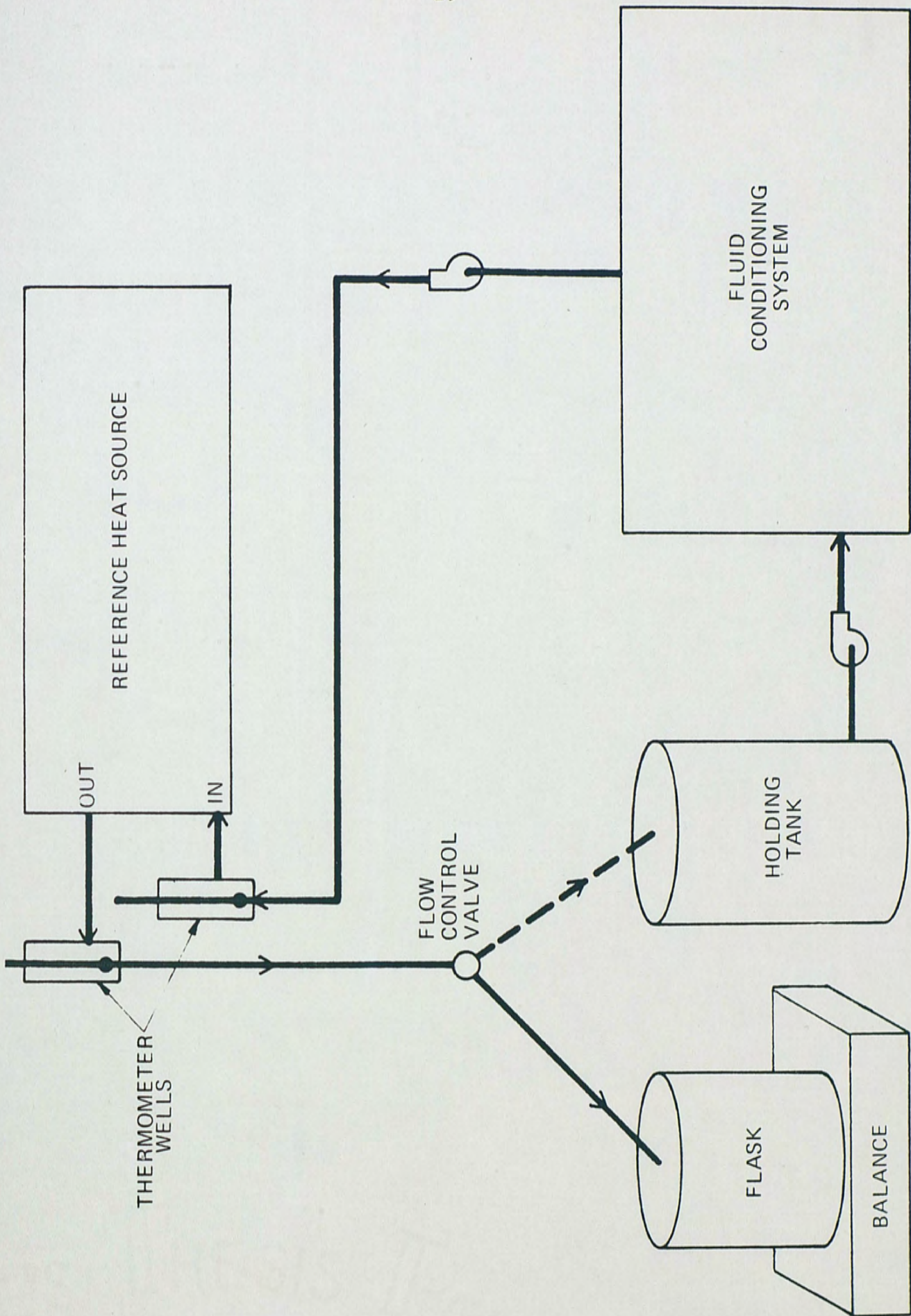


Fig. 9. Operational Calibration Schematic

The results of the tests with no electrical input to the core heaters were used to determine the heat loss from the core as a function of the temperature difference between the fluid and the ambient air. The temperature of the fluid was controlled with the test facility's fluid conditioning equipment. Figure 10 presents the results for two operating conditions. Detailed data from the heat loss tests is presented in Appendix 3. The heat loss rate was measured with and without the thermal shield operating. Without the shield, the heat loss rate was approximately 0.8 watts/°C. Part of the loss is through the core insulation and part is through the connecting hoses and thermometer wells. With the shield, the heat loss rate drops to approximately 0.2 watts/°C. Ideally, with the shield operational, the heat loss from the core would be zero if enough time has been allowed for thermal stabilization of the core and its insulation. It was not clear at this point whether the measured loss was through the shield or through connecting hoses and thermometer wells. It was observed that time required for stabilization (constant outlet temperature once a constant inlet temperature had been established) was approximately 10 to 15 minutes with the shield operational and approximately one hour without it. During use of the RHS, the thermal shield should prove to be a distinct advantage in reducing the time required to complete any test sequence.

A time constant test was conducted to determine the thermal time response of the RHS. In this test a stable operating configuration was obtained with the temperature of the fluid entering

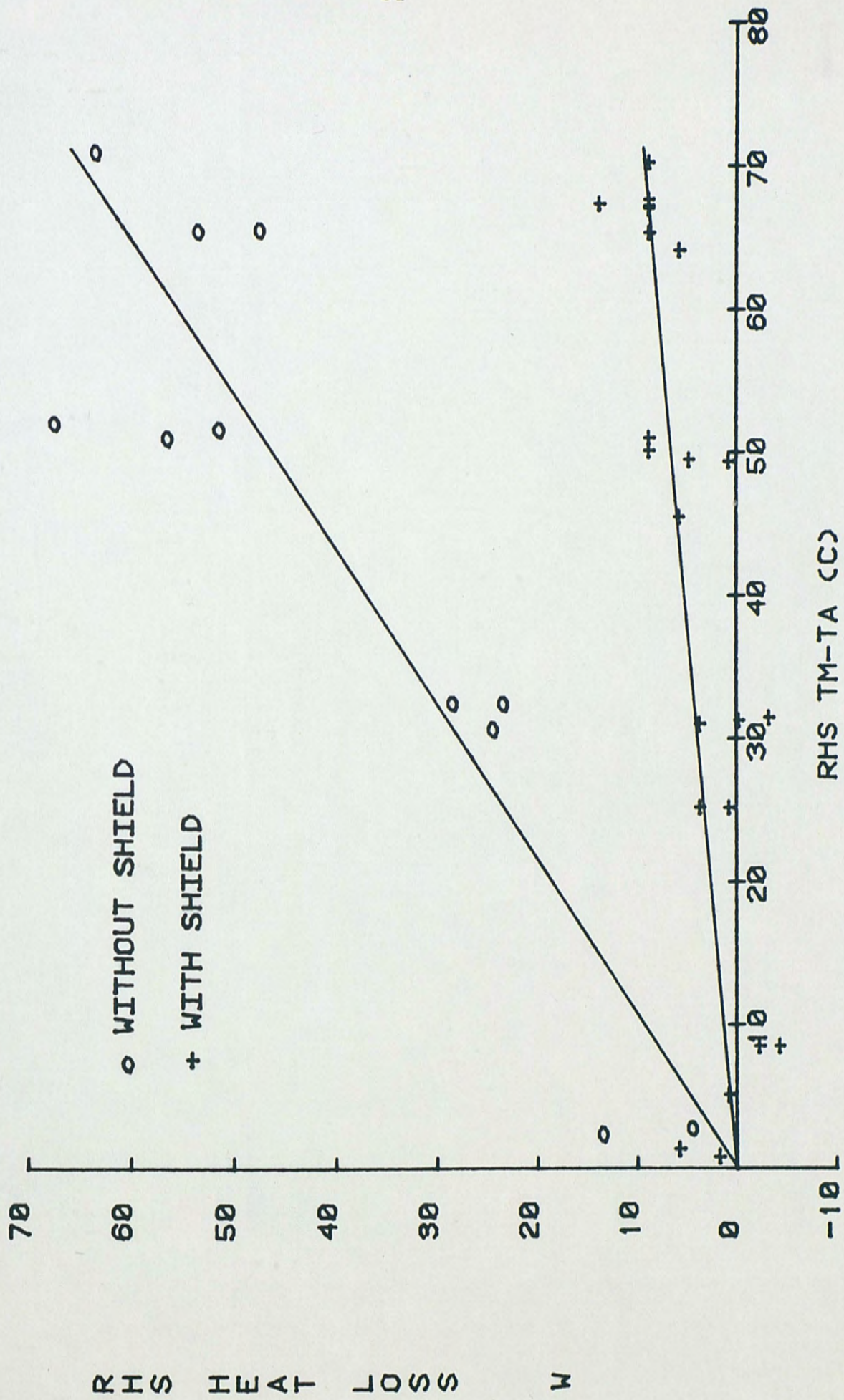


Fig. 10. Heat loss from the core as a function of operating temperature and thermal shield operation

the RHS set 10°C above the ambient air temperature. The flow rate was approximately 0.06 kg/sec and all four elements (\cong 1800 watts) were turned on. At time zero, the heating elements were turned off. The outlet temperature was monitored while the inlet temperature and flow rate were held constant. The thermal shield was operating. Figure 11 presents a plot of the difference between the inlet and outlet temperatures versus time. This gives an indication of the thermal lag due to the mass of the RHS itself which must be considered when attempting to reach a stable operating condition.

The third graph, presented in Figure 12, presents the RHS efficiency as a function of the difference in temperature between the fluid and the ambient air. This efficiency is defined as the ratio of the thermal energy removed from the core (as measured by the calibration standards) to the electrical power added to the core heaters (as measured by the RHS power transducer):

$$\eta_{\text{RHS}} = \frac{Q_{\text{STD}}}{Q_{\text{RHS}}} \quad (12)$$

where

Q_{STD} = thermal output of RHS as measured by the calibration standards

Q_{RHS} = electrical energy input to the RHS core heaters
as measured by the RHS power transducer.

The thermal output of the RHS, Q_{STD} , is calculated from the measurements made by the calibration standards

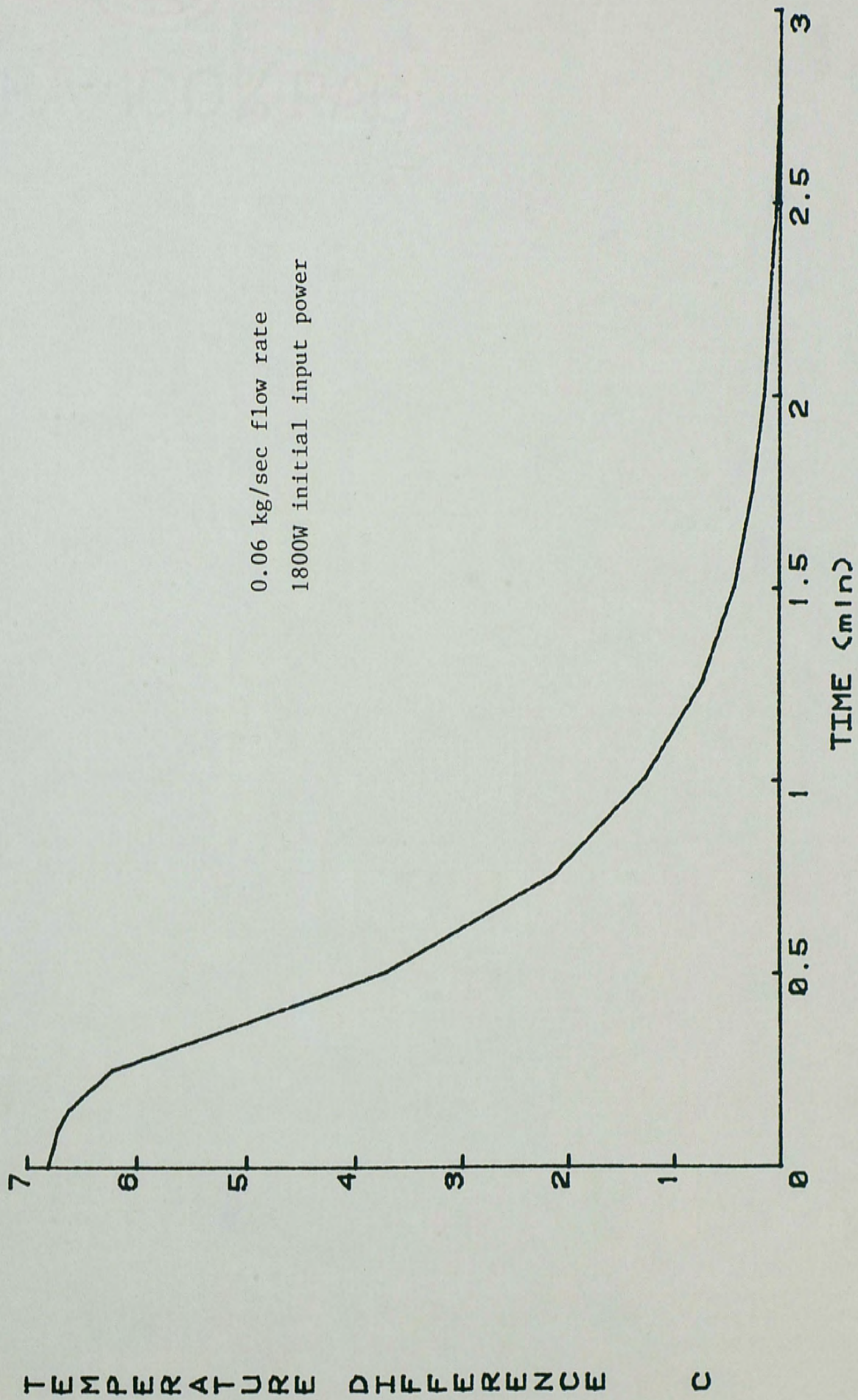


Fig. 11. Time Constant

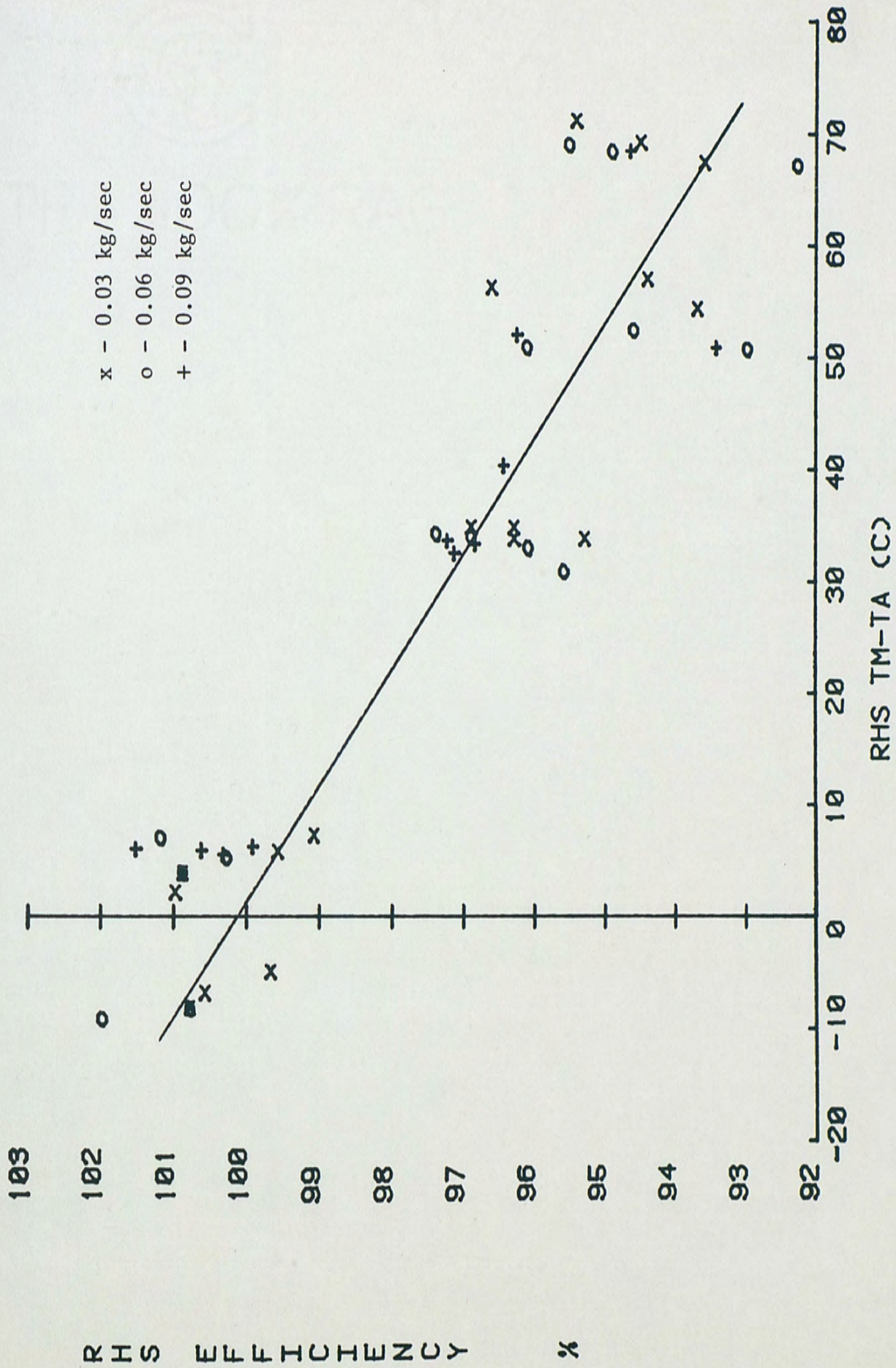


Fig. 12. Initial operational calibration of RHS efficiency as a function of operating temperature

$$Q_{STD} = m_{STD} C_p \Delta T_{STD} \quad (13)$$

where

m_{STD} = mass flow rate through the RHS core as determined by gravimetric measurement

C_p = specific heat of the fluid determined from the standard values for water as a function of temperature

ΔT_{STD} = difference in temperature of the fluid between the inlet and outlet of the RHS as measured by the calibration mercury in glass thermometers

This efficiency represents the accuracy with which the electrical input is measured and the effectiveness of the thermal shield in preventing heat loss from the core. The efficiency was measured over the range of flow rates, temperatures, and power settings mentioned previously. Detailed data from the efficiency tests is presented in Appendix 3.

During calibration, all operating conditions were maintained as stable as possible. The inlet temperature was controlled to $\pm 0.3^\circ\text{C}$. Stability of $\pm 0.1^\circ\text{C}$ would have been desirable to make the calibration easier to accomplish. The electrical supply voltage was generally stable to ± 0.2 volts. Occasional changes of up to one volt made it necessary to wait for the temperature to stabilize again. The use of a regulated power supply would be advisable to

prevent this and to improve accuracy during test facility verification and collector testing. The flow rate was maintained within $\pm 0.5\%$ by monitoring the output of a turbine meter. The thermal shield was typically maintained within $\pm 0.5^\circ\text{C}$ of the core temperature. The scatter in the calibration data was found to have been due primarily to instability in two operating parameters: inlet fluid temperature and electrical supply voltage.

During calibration at the high temperature of ambient air temperature plus 70°C , the outlet temperature rose above 100°C . At this point it was discovered that since the water in the shield loop was at atmospheric pressure, it would have to be replaced with an antifreeze mixture to raise its boiling temperature above 100°C . With plain water in the shield loop, boiling resulted in vapor locks which stopped the flow and eliminated the effectiveness of the shield in preventing heat loss from the core.

During these calibrations, it was also discovered that the thermopile was damaged badly enough in an earlier accident that it would have to be replaced. Its output is included in the computer print-outs presented in Appendix 3 in anticipation of obtaining a new thermopile to use as a verification of the temperature rise indicated by the platinum resistance thermometers.

In an attempt to reduce the heat loss and improve the efficiency of the RHS, the length of the connecting hoses was shortened to 25 cm and changed to copper tubing insulated with 5.1 cm of elastomeric thermal insulating foam. Another calibration was conducted. This time only one flow rate (0.06 kg/sec) and three

input power levels (0, 1000, and 2000 watts) were investigated. A more accurate beam balance (accurate to ± 0.02 kilograms) was used for this series of calibration tests.

The results of the heat loss tests, conducted during the second calibration showed a reduction in heat loss compared to the first calibration, indicating that the majority of the losses were through the thermometer wells and fluid line connections. The RHS efficiency, presented in Figure 13, showed considerable improvement compared to the initial calibration.

This final calibration was used to develop a correction factor equation for the RHS. This is a linear least squares curve to fit to the data in figure 13. The correction is applied to the electrical power input when the RHS is used in its two normal modes of operation. This correction accounts for the losses and inaccuracies found during calibration:

$$\eta_{\text{CAL}} = 0.998 - 0.00052 (T_m - T_a) \quad (14)$$

where

η_{CAL} = correction factor to be multiplied by the indicated RHS electrical input power to determine the true thermal output of the RHS

T_m = average of the RHS inlet and outlet temperature sensors in $^{\circ}\text{C}$

T_a = ambient air temperature in $^{\circ}\text{C}$

Details of the calibration tests are presented in Appendix 3 along with column heading definitions. Both the heat loss and

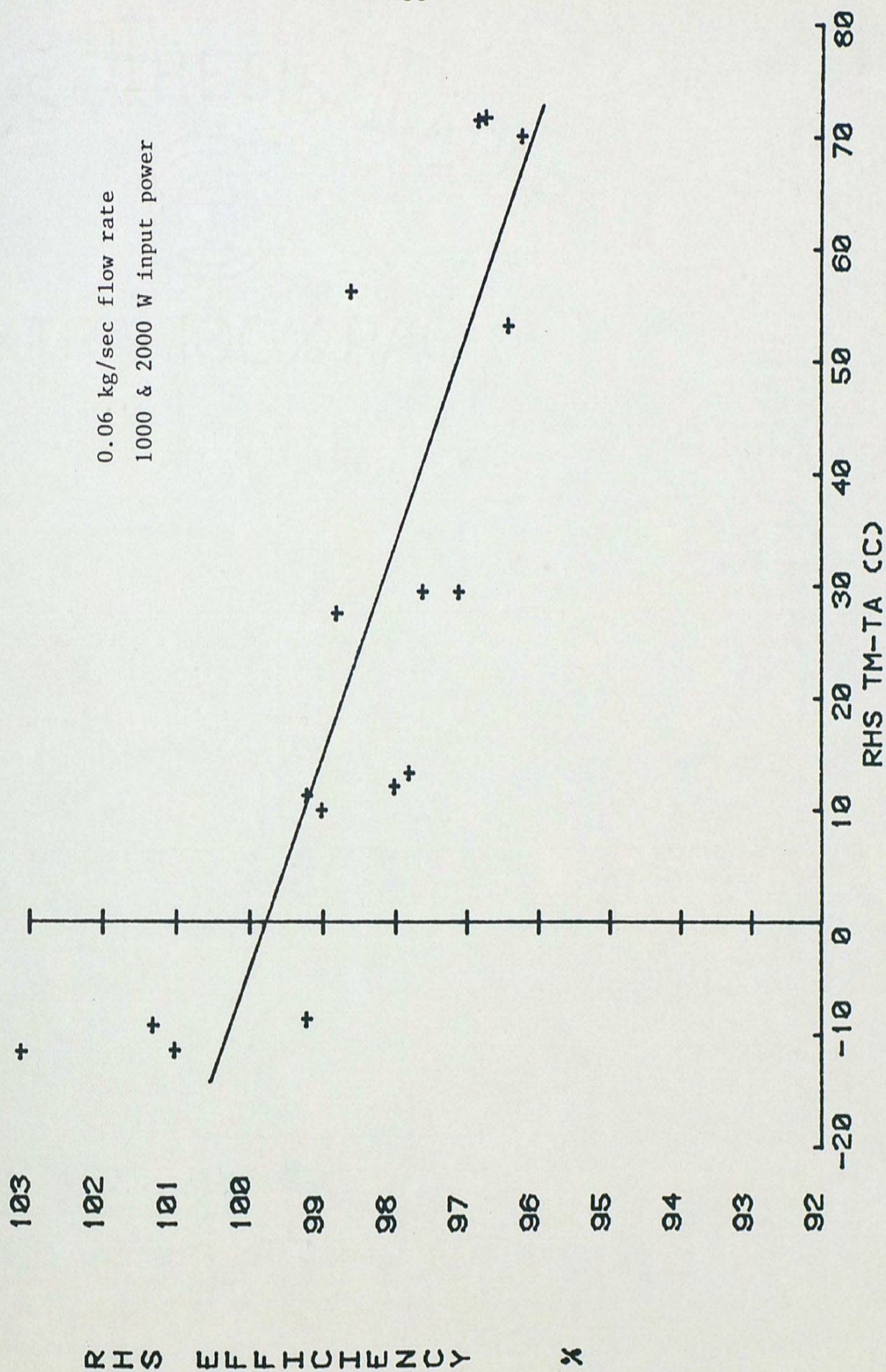


Fig. 13. Final operational calibration of RHS efficiency as a function of operating temperature

efficiency test runs for both calibrations are included. Periodic re-running of these calibrations should be conducted to insure the accuracy of the RHS at all times.

CHAPTER V

OPERATION

The RHS can be used in two distinctly different operating modes. These two modes, also discussed in Chapter I, are test facility calibration verification and solar collector testing. The primary use of this particular RHS has been in calibration verification because of the accuracy precautions taken in its design and construction. Additional studies have been conducted and future work is planned to investigate the use of the RHS concept in full time solar collector testing.

Test Facility Verification

The RHS can be substituted for a solar collector in the test facility as illustrated in Figure 1. In this mode, the calibration of the facility's temperature and flow sensors are verified as are the calculation procedures used to determine the energy output of a collector. A specific amount of energy is added to the fluid as it passes through the RHS. Since this quantity of energy is accurately measured by the RHS, the accuracy of the test facility's determination of the output can be verified. The accuracy of the fluid temperature sensors is also verified at the same time by direct comparison. The heat loss from the lines between the facility and the RHS must be minimized as discovered during calibration.

The insulating materials and techniques normally used during collector testing are also employed here to determine if there is excessive heat loss which would lower the indicated performance of a solar collector under test.

Any difference between the RHS input power and the facility's measurements requires determination of the source of the error. The error in the facility's output measurement is presented as recommended by Jenkins and Streed [12] and discussed in Chapter 1. The percentage error is plotted versus the difference between the mean fluid temperature and the ambient air temperature. From this, the operating conditions at which errors occur are easily identified.

The RHS was used to check the calibration of several solar collector test stands at the Florida Solar Energy Center. The results of one facility-verification run are presented in Figure 14. This particular run was conducted with a turbine flow meter having an output that decreased with increasing temperature to demonstrate the resulting increase in error. Data was collected at a flow rate of 0.06 kilograms per second. The fluid temperature was set equal to the ambient air temperature as well as 30, 50, and 70°C above the air temperature. It can be observed that the test facility's measurement was consistently one to five percent low.

The results of a second facility-verification run are presented in Figure 15. This test stand exhibited accuracy within one percent at all operating temperatures except the highest where the error increased to just over one and one-half percent. The source

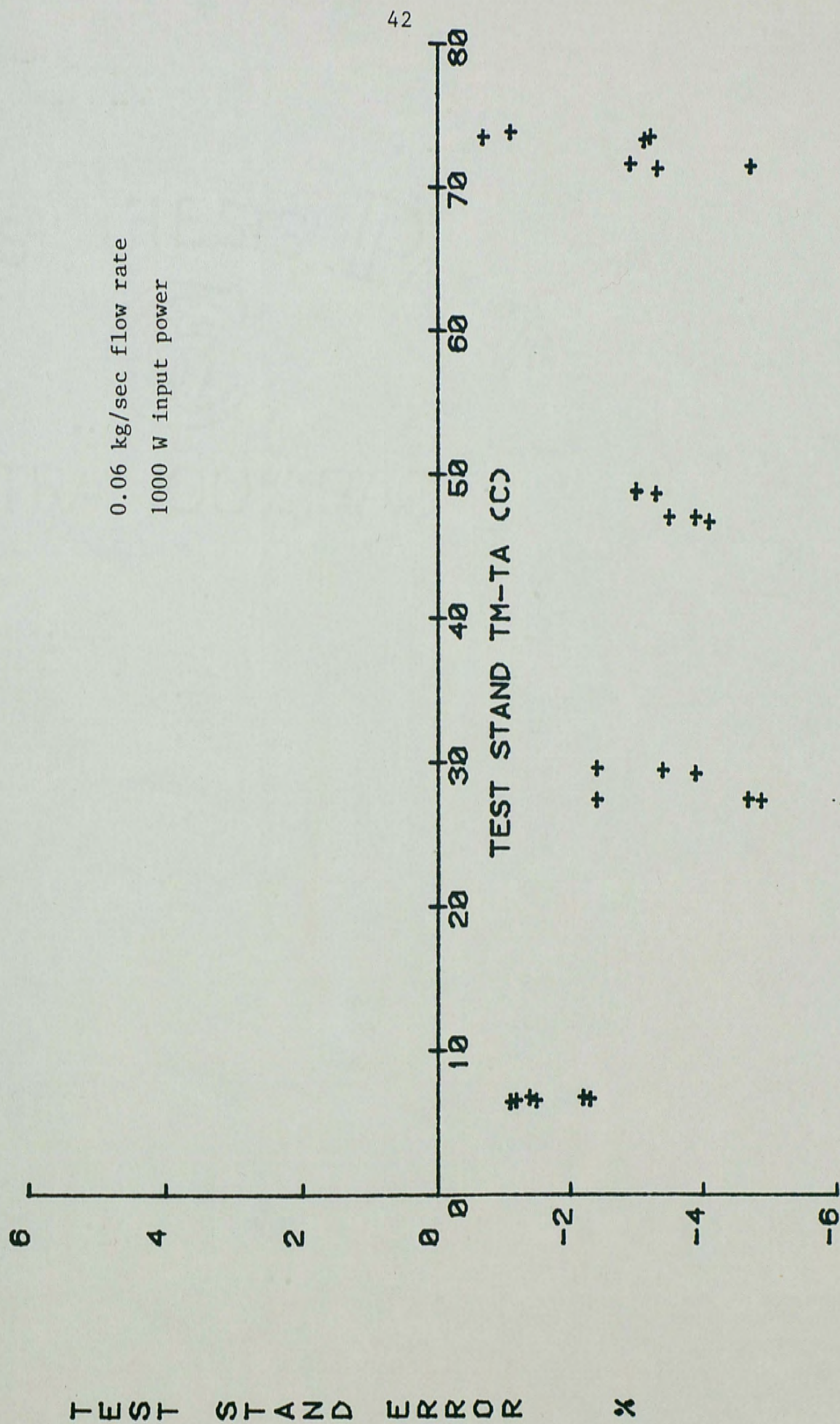


Fig. 14. Sample test facility verification results showing error due to an inaccurate flow meter

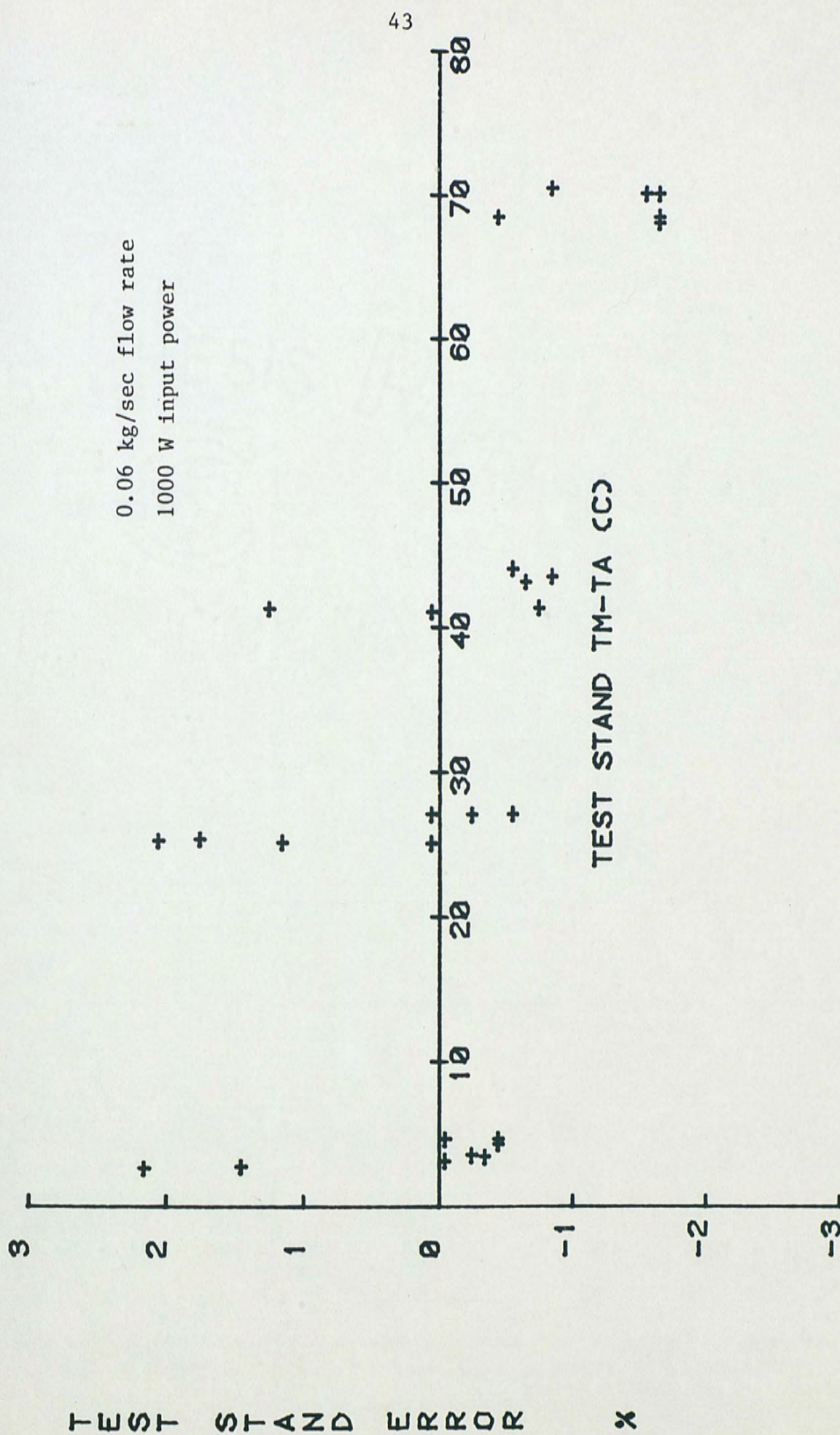


Fig. 15. Sample test facility verification results showing scatter due to unstable operating conditions

of the error was again found to be in the turbine flow meter system. The data points scattered above a one percent error were the result of lack of stability in either the flow rate or fluid temperature supplied by the test facility or were due to a sudden change in the voltage of the electrical supply to the RHS. In normal collector testing these points would simply be discarded on the basis of nonstable operating conditions.

Periodic runs of this type are conducted to insure that the highest possible accuracy is maintained on all of the solar collector test stands. During these verification runs, the driven shield proved to be especially useful in reducing the time required to stabilize after a change in operating temperature. The time required to restabilize was typically 10 to 15 minutes following a 20°C change in core temperature. With the shield loop turned off, this time was often more than an hour.

Detailed data from these test facility verification runs are presented in Appendix 4.

Solar Collector Testing

To determine the output of a solar collector, the RHS is placed ahead of and in series with the collector as shown in Figure 2. The transfer fluid thus passes through the RHS and then the collector at exactly the same mass flow rate. A number of error sources are eliminated in this mode of operation: flow rate measurement errors, specific heat and density calculations or table

interpolations, and heat loss in lines to and from the RHS. Determination of the energy output from the collector reduces to the simple ratio defined in equation (6):

$$Q_{\text{COLLECTOR}} = Q_{\text{RHS}} \frac{\Delta T_{\text{COLLECTOR}}}{\Delta T_{\text{RHS}}}$$

Limited experience with the RHS in this mode has been obtained. It is anticipated, however, that this will be a quite accurate means of determining the output of a solar collector. Tests conducted on typical glazed, liquid, flat plate collectors have shown agreement within two percent between the RHS method and a very carefully conducted conventional test. It is important to note that the RHS does not eliminate the need to measure the solar irradiance in this mode. Obtaining the thermal efficiency will still depend on separate measurement of the solar irradiance in the plane of the collector. Full scale implementation of the RHS in this mode would require the development of a more permanent device with instrumentation outputs interfaced directly with the test facility data acquisition system.

CHAPTER VI

CONCLUSIONS

The use of an electrical calorimeter in a solar collector test facility appears to have a number of advantages. The reference heat source concept provides a multipurpose device capable of easing several of the complicated measurements that are required. The RHS is useful in both verifying test facility calibrations and in testing solar collectors.

In the application of calibration verification, the RHS provides a relatively rapid means of confirming the instrumentation in a test facility. The RHS developed here is a portable device that can easily be moved to each test stand. The temperature and flow rate measurements of the test facility can be checked against the instrumentation in the RHS. Periodic (yearly) recalibration of the RHS itself insures continued accuracy.

The second application involves the use of the RHS concept in routine solar collector testing operations. Here, the RHS allows elimination of several measurements and procedures which introduce considerable error into the collector performance determination. The elimination of the mass flow rate measurement is the greatest advantage. The RHS developed here can be used in this manner, however, since it was designed primarily as a calibration tool, its

application to collector testing is limited to verifying the validity of the technique. RHS devices for each test stand with recorded instrumentation outputs must be developed for full-scale implementation in this mode.

The use of a driven thermal shield to control heat loss from the core of the RHS was found to have at least two significant advantages. First, it effectively controlled the heat loss better than any technique previously reported. By isolating the core from environment, the effect of random changes in air temperature, wind velocity, and solar irradiance were minimized. Second, the driven shield reduced the time required to reach stable operating conditions. This proved to be a significant operational advantage in both modes of use. With the shield operating, the RHS does not lag behind the remainder of the test system. Without the shield, the RHS delays any other operations which might be in progress.

Finally, the RHS that has been developed and reported on here leads to the recommendation that this concept, particularly with the incorporation of a driven thermal shield, be further utilized in both of its operational modes in all solar collector testing operations.

REFERENCES

1. American Society of Heating, Refrigerating, and Air-Conditioning Engineers. Methods of Testing to Determine the Thermal Performance of Unglazed Flat-Plate Liquid Type Solar Collectors, ASHRAE Standard 96-1980. New York: American Society of Heating, Refrigerating, and Air-Conditioning Engineers, 1980.
2. American Society of Heating, Refrigerating, and Air-Conditioning Engineers. Methods of Testing to Determine the Thermal Performance of Solar Collectors, ASHRAE Standard 93-77. New York: American Society of Heating, Refrigerating, and Air-Conditioning Engineers, 1977.
3. Thomas, Carl C. "The Measurement of Gases." Journal of the Franklin Institute 172 (November 1911): 411-460.
4. Benson, James M. "Survey of Thermal Devices for Measuring Flow." In Flow - It's Measurement and Control in Science and Industry, Vol. 1, part 2, Edited by R.E. Wendt. Pittsburgh: Instrument Society of America, 1974.
5. Gillett, W.B.; and Rawcliffe, R.W. Calorimetric Test Facility Calibration. Departmental Report No. 471, SEU No. 106, Cardiff, Great Britain, 1980.
6. Bougard, J.; Pilatte, A.; and Lagneau, V. "Calibration of a Calorimetric Flowmeter." Center for Research of Solar Energy, Mons, Belgium, n.p. 1980.
7. Carroll, J., and Wald, D. "Performance Testing of Solar Collectors." n.p., Santa Clara, CA, 1979.
8. Reed, Kent A., and Allen, John W. "Solar Thermal Collector Testing: Calorimetric Ratio Technique." Proceedings of the 1978 Annual Meeting. Newark, Delaware: American Section of the International Solar Energy Society, 1978.
9. Jenkins, John P. The Design and Evaluation of a Reference Heat Source to be Used in Conjunction with Solar Collector Testing. Washington, D.C.: National Bureau of Standards, 1979.
10. Anderson, Hans E.B. "IEA Task III, Reference Heat Source, A Discussion." Great Britain: International Energy Agency, 1980. (Typewritten.)

11. Collares-Pereira, M.; Duque, J.; Saraiva, C.; and Rego-Teixeira, A. "A Calorimeter for Solar Thermal Collector Testing." Solar Energy 27 (1981): 581-582.
12. Jenkins, John P., and Streed, Elmer R. Comments and Suggestions for Reference Heat Source Calibration and Operation Format. Washington, D.C.: National Bureau of Standards, 1980.
13. Clinton, James R. "An Electrical Calorimeter for Collector Test Facility Calibrations." San Diego: Solar Energy Analysis Laboratory, n.p. 1981.
14. Doebelin, Ernest O. Measurement Systems. New York: McGraw-Hill Book Company, 1975.
15. Streed, Elmer R., and Waksman, David. "NBS Solar Collector Durability/Reliability Program," pp. 239-249. In Durability of Building Materials and Components, ASTM STD 691. Edited by P.J. Sereda and G.G. Litvan. New York: American Society for Testing and Materials, 1980.

APPENDICES

APPENDIX 1

RHS INSTRUMENTATION SPECIFICATIONS

Digital Panel Meters:

IMC model 60001

Range:	0-199.99 mV
Accuracy:	$\pm 0.01\%$ of span
Output:	4½ digit LED

Platinum Resistance Thermometers:

Omega Model 100R30

Nominal resistance:	100 ohms
Response time:	0.15 seconds
Stability:	$\pm 0.1\%$

PRT Linear Bridge:

Rosemont Model 414L

Range:	-100°C to +200°C
Accuracy:	$\pm 0.2^\circ\text{C}$
Output:	1 mV/°C
Nonlinearity:	$\pm 0.03\%$ (max.)

Power Transducer:

F.W. Bell Model PR2101S

Range: 0 to 500 watts

Accuracy: 0.5% of span

Response time: 0.4 seconds

Power factor correction: automatic

Thermopile:

Delta-T Model Differential Temperature Transducer

Sensitivity: 0.223 mV/°F differential

Accuracy: $\pm 0.07^\circ\text{F}$

Response time: 0.5 seconds

APPENDIX 2

CALIBRATION STANDARDS SPECIFICATIONS

Voltage Standard:*

Fluke Model 335D

Output voltage:	0 to 111.1110 VDC
Output current:	0 to 50 milliamperes
Resolution:	1 microvolt
Accuracy:	± 10 microvolts

Temperature Calibration Bath:

Rosemont Model 910A

Temperature range:	-60°C to +260°C
Temperature uniformity:	$\pm 0.006^\circ\text{C}$
Stability:	$\pm 0.006^\circ\text{C}/\text{hour}$

Mercury in Glass Thermometers:*

Brooklyn Thermometer Model Calorimeter Thermometer

Accuracy:	$\pm 0.01^\circ\text{C}$
Resolution:	0.01°C

Electrical Shunt:*

Weston Model KS9442-L1

Resistance:	$0.003364377 \pm 1.0 \times 10^{-9}$ ohm
-------------	--

Differential Voltmeter:*

Fluke model 887A

Range: 0 to 10999.999V

Resolution: 1 microvolt

Multimeter:

Fluke Model 8020A

Range: 0 to 1000 VDC

Resoltuion: $\pm 0.1V$

Oscilloscope:

Phillips Model PM3218

Frequency limit: 35MHz

Voltage resolution: 2 mV/cm

Beam Scale:*

Chatillon Model PBB-135

Range: 0-135 pounds

Resoltuion: 1 ounce

* These instruments have calibrations directly traceable to NBS standards.

APPENDIX 3

RHS CALIBRATION

COMPUTER PRINTOUT KEY

DATE	-	Date of the test run
TIME	-	Eastern standard time
STD IN	-	Temperature of the fluid at the inlet of the RHS as measured by a mercury in glass thermometer in °C
STD OUT	-	Temperature of the fluid at the outlet of the RHS as measured by a mercury in glass thermometer in °C
STD DELTA	-	Difference between the fluid inlet and outlet temperatures as measured by the mercury in glass thermometers in °C.
GRAV FLOW	-	Mass flow rate of the fluid through the RHS core as measured by a beam scale and a stop watch in kilograms per second.
RHS IN	-	Temperature of the fluid at the inlet of the RHS as measured by the RHS inlet platinum resistance thermometer in °C
RHS OUT	-	Temperature of the fluid at the outlet of the RHS as measured by the RHS outlet platinum resistance thermometer in °C.

- RHS DELTA - Difference between the fluid inlet and outlet temperatures as measured by the RHS platinum resistance thermometers in °C.
- TPILE DELTA - Difference between the fluid inlet and outlet temperatures as measured by the thermopile in °C
- RHS PWR - Electrical power input to the RHS core heaters as measured by the RHS power transducer in watts
- AIR TEMP - Temperature of the ambient air in the vicinity of the RHS as measured by a shielded, aspirated platinum resistance thermometer in °C.
- STD OUTPUT - Thermal output of the RHS as measured by the calibration standards
- RHS FLOW - Mass flow rate of fluid through the RHS core as determined from measurements by RHS instrumentation.
- DLTA ERR - Error in temperature rise indicated by RHS instrumentation as compared to the calibration standards:
$$ERR = \frac{(RHS \text{ DELTA} - STD \text{ DELTA}) * 100}{STD \text{ DELTA}}$$

- FLOW ERR - Error in mass flow rate determined by the RHS as compared to the gravimetric flow rate measurement: $ERR = (RHS\ FLOW - GRAV\ FLOW) * 100 / GRAV\ FLOW$
- RHS TM-TA - Difference in temperature between the average fluid temperature, as measured by the RHS, and the ambient air temperature in °C: $\frac{1}{2}(RHS\ IN + RHS\ OUT) - AIR\ TEMP$
- RHS EFF - RHS efficiency as defined in Chapter I
- EFF UNCR POSS - Maximum possible uncertainty in the RHS efficiency measurements in $\pm\%$.
- EFF UNCR PRBL - Probable uncertainty in the RHS efficiency measurement in $\pm\%$.
- RHS LOSS - Heat loss from the RHS as measured by the calibration standards in watts.
- LOSS POSS - Maximum possible uncertainty in the RHS heat loss measurement in \pm watts.
- LOSS PRBL - Probable uncertainty in the RHS heat loss measurement in \pm watts.

DATE	TIME	STD IN C	STD OUT C	STD DELTA C	GRAV FLOW kg/sec	RHS IN C	RHS OUT C	RHS DELTA C	RHS IPILE DELTA C	RHS PWR W	AIR TEMP C	STD OUTPUT W	RHS FLOW kg/sec	DLTA ERR Z	FLOW ERR Z	RHS TA-TA C	RHS EFF Z	RHS EFF UNCOR PRBL	RHS LOSS W	LOSS POSS +/-W	LOSS PRBL +/-W
3/18/82	12:14	30.43	30.42	-0.01	0.0958	30.46	30.45	-0.01	0.01	3.28.1	3.28.1	-4.	0.0000	-0.0	0.0000	2.35	0.0000	0.0000	4.	12.1	8.6
3/18/82	12:12	30.49	30.44	-0.05	0.0633	30.56	30.53	-0.03	0.01	4.28.6	4.28.6	-13.	0.0000	0.0000	0.0000	1.94	0.0000	0.0000	13.	7.9	5.7
3/17/82	16:52	58.65	58.48	-0.17	0.0323	58.49	58.49	0.00	0.03	3.26.7	3.26.7	-23.	0.0000	0.0000	0.0000	31.79	0.0000	0.0000	23.	3.9	2.9
3/19/82	11:09	59.12	59.03	-0.09	0.0631	59.14	59.10	-0.04	0.06	3.29.1	3.29.1	-24.	0.0000	0.0000	0.0000	30.02	0.0000	0.0000	24.	7.7	5.6
3/19/82	15:44	59.87	59.80	-0.07	0.0944	59.79	59.82	0.03	0.14	3.28.0	3.28.0	-28.	0.0000	0.0000	0.0000	31.81	0.0000	0.0000	28.	11.5	8.4
3/15/82	16:51	77.85	77.35	-0.50	0.0319	77.61	77.51	-0.10	-0.03	4.26.4	4.26.4	-67.	0.0000	0.0000	0.0000	51.16	0.0000	0.0000	67.	3.5	2.9
3/16/82	9:18	76.40	76.19	-0.21	0.0635	76.29	76.24	-0.05	-0.03	3.26.2	3.26.2	-56.	0.0000	0.0000	0.0000	50.06	0.0000	0.0000	56.	7.5	5.7
3/16/82	16:34	77.74	77.61	-0.13	0.0937	77.64	77.60	-0.04	0.01	3.26.9	3.26.9	-51.	0.0000	0.0000	0.0000	50.72	0.0000	0.0000	51.	11.2	8.3
3/19/82	19:31	93.49	93.33	-0.16	0.0928	93.26	93.24	-0.02	0.03	4.23.3	4.23.3	-63.	0.0000	0.0000	0.0000	69.95	0.0000	0.0000	63.	11.0	8.3
3/20/82	19:06	89.74	89.54	-0.20	0.0631	89.56	89.55	-0.01	0.08	4.25.1	4.25.1	-53.	0.0000	0.0000	0.0000	64.46	0.0000	0.0000	53.	7.4	5.6
3/20/82	22:34	89.60	89.25	-0.35	0.0320	89.33	89.30	-0.03	0.00	4.24.8	4.24.8	-47.	0.0000	0.0000	0.0000	64.51	0.0000	0.0000	47.	3.6	2.9

Fig. 16. Heat Loss Data Without Shield

DATE	TIME	STD IN	STD OUT	STD DELTA	GRAV FLOW	RHS IN	RHS OUT	RHS DELTA	RHS TPILE	RHS CALIBRATION										RHS TA-TA	RHS Z	DLTA ERR	FLOW ERR	RHS Z	RHS TA-TA	RHS Z	EFF UNCOR	EFF POSS	RHS LOSS	LOSS POSS	PRBL +/-W	LOSS PRBL +/-W
										C	C	C	C	C	C	C	C	C	C	C	C	C	C	C	C	C	C	C	C	C	C	C
3/17/82	17:23	29.15	29.15	-0.00	0.0309	29.23	29.22	-0.01	0.03	-7.28.8	-0.03	0.03	0.03	0.03	0.03	0.03	0.03	0.03	0.03	0.03	0.03	0.03	0.03	0.03	0.03	0.03	0.03	0.03	0.03	0.03	0.03	0.03
3/18/82	13:12	30.58	30.61	0.03	0.0638	30.66	30.64	-0.02	0.11	3.29.7	-0.11	0.11	0.11	0.11	0.11	0.11	0.11	0.11	0.11	0.11	0.11	0.11	0.11	0.11	0.11	0.11	0.11	0.11	0.11	0.11	0.11	0.11
3/18/82	16:33	30.57	30.60	0.03	0.0945	30.62	30.62	0.00	0.07	4.25.9	0.07	0.07	0.07	0.07	0.07	0.07	0.07	0.07	0.07	0.07	0.07	0.07	0.07	0.07	0.07	0.07	0.07	0.07	0.07	0.07	0.07	0.07
3/17/82	15:49	58.60	58.42	-0.18	0.0329	58.51	58.52	0.01	0.08	4.27.7	0.08	0.08	0.08	0.08	0.08	0.08	0.08	0.08	0.08	0.08	0.08	0.08	0.08	0.08	0.08	0.08	0.08	0.08	0.08	0.08	0.08	0.08
3/19/82	11:30	59.48	59.37	-0.11	0.0634	59.42	59.41	-0.01	0.07	3.28.9	0.07	0.07	0.07	0.07	0.07	0.07	0.07	0.07	0.07	0.07	0.07	0.07	0.07	0.07	0.07	0.07	0.07	0.07	0.07	0.07	0.07	0.07
3/19/82	15:1	59.76	59.66	-0.10	0.0944	59.68	59.69	0.01	0.09	3.28.7	0.09	0.09	0.09	0.09	0.09	0.09	0.09	0.09	0.09	0.09	0.09	0.09	0.09	0.09	0.09	0.09	0.09	0.09	0.09	0.09	0.09	0.09
3/15/82	15:58	78.12	77.75	-0.37	0.0318	77.90	77.84	-0.06	0.06	4.27.4	0.06	0.06	0.06	0.06	0.06	0.06	0.06	0.06	0.06	0.06	0.06	0.06	0.06	0.06	0.06	0.06	0.06	0.06	0.06	0.06	0.06	0.06
3/20/82	13:45	78.90	78.75	-0.15	0.0626	78.85	78.83	-0.02	0.08	3.33.8	0.08	0.08	0.08	0.08	0.08	0.08	0.08	0.08	0.08	0.08	0.08	0.08	0.08	0.08	0.08	0.08	0.08	0.08	0.08	0.08	0.08	0.08
3/16/82	13:36	78.07	77.96	-0.11	0.0948	77.99	77.98	-0.01	0.13	3.29.0	0.13	0.13	0.13	0.13	0.13	0.13	0.13	0.13	0.13	0.13	0.13	0.13	0.13	0.13	0.13	0.13	0.13	0.13	0.13	0.13	0.13	0.13
3/20/82	22:49	89.40	89.18	-0.22	0.0322	89.17	89.13	-0.04	0.00	4.25.5	0.00	0.00	0.00	0.00	0.00	0.00	0.00	0.00	0.00	0.00	0.00	0.00	0.00	0.00	0.00	0.00	0.00	0.00	0.00	0.00	0.00	0.00
3/20/82	19:22	89.90	89.72	-0.18	0.0630	89.75	89.72	-0.03	0.06	4.24.9	0.06	0.06	0.06	0.06	0.06	0.06	0.06	0.06	0.06	0.06	0.06	0.06	0.06	0.06	0.06	0.06	0.06	0.06	0.06	0.06	0.06	0.06
3/19/82	19:50	93.33	93.20	-0.13	0.0932	93.18	93.16	-0.02	0.04	4.23.4	0.04	0.04	0.04	0.04	0.04	0.04	0.04	0.04	0.04	0.04	0.04	0.04	0.04	0.04	0.04	0.04	0.04	0.04	0.04	0.04	0.04	0.04
5/1/82	13:20	34.77	34.80	0.03	0.0571	34.80	34.82	0.02	0.05	3.26.7	0.05	0.05	0.05	0.05	0.05	0.05	0.05	0.05	0.05	0.05	0.05	0.05	0.05	0.05	0.05	0.05	0.05	0.05	0.05	0.05	0.05	0.05
5/1/82	13:51	35.03	35.03	-0.00	0.0629	35.06	35.07	0.01	0.07	3.26.9	0.07	0.07	0.07	0.07	0.07	0.07	0.07	0.07	0.07	0.07	0.07	0.07	0.07	0.07	0.07	0.07	0.07	0.07	0.07	0.07	0.07	0.07
5/8/82	21:57	49.75	49.64	-0.11	0.0631	49.71	49.71	-0.00	0.01	3.25.0	0.01	0.01	0.01	0.01	0.01	0.01	0.01	0.01	0.01	0.01	0.01	0.01	0.01	0.01	0.01	0.01	0.01	0.01	0.01	0.01	0.01	0.01
5/8/82	22:7	49.77	49.65	-0.12	0.0630	49.72	49.71	-0.01	0.01	3.25.0	0.01	0.01	0.01	0.01	0.01	0.01	0.01	0.01	0.01	0.01	0.01	0.01	0.01	0.01	0.01	0.01	0.01	0.01	0.01	0.01	0.01	0.01
5/1/82	18:10	73.08	73.00	-0.08	0.0628	73.00	73.00	0.00	0.05	3.24.1	0.05	0.05	0.05	0.05	0.05	0.05	0.05	0.05	0.05	0.05	0.05	0.05	0.05	0.05	0.05	0.05	0.05	0.05	0.05	0.05	0.05	0.05
5/1/82	18:22	73.61	73.40	-0.21	0.0627	73.48	73.45	-0.03	0.01	3.23.8	0.01	0.01	0.01	0.01	0.01	0.01	0.01	0.01	0.01	0.01	0.01	0.01	0.01	0.01	0.01	0.01	0.01	0.01	0.01	0.01	0.01	0.01
5/9/82	0:48	90.70	90.56	-0.14	0.0625	90.57	90.52	-0.05	0.04	3.23.7	0.04	0.04	0.04	0.04	0.04	0.04	0.04	0.04	0.04	0.04	0.04	0.04	0.04	0.04	0.04	0.04	0.04	0.04	0.04	0.04	0.04	0.04
5/9/82	1:5	90.50	90.37	-0.13	0.0629	90.35	90.32	-0.03	0.03	4.23.8	0.03	0.03	0.03	0.03	0.03	0.03	0.03	0.03	0.03	0.03	0.03	0.03	0.03	0.03	0.03	0.03	0.03	0.03	0.03	0.03	0.03	0.03
5/9/82	1:21	90.52	90.44	-0.08	0.0625	90.42	90.39	-0.03	0.04	3.23.7	0.04	0.04	0.04	0.04	0.04	0.04	0.04	0.04	0.04	0.04	0.04	0.04	0.04	0.04	0.04	0.04	0.04	0.04	0.04	0.04	0.04	0.04
5/9/82	1:49	90.29	90.20	-0.09	0.0626	90.18	90.15	-0.03	0.05	4.23.1	0.05	0.05	0.05	0.05	0.05	0.05	0.05	0.05	0.05	0.05	0.05	0.05	0.05	0.05	0.05	0.05	0.05	0.05	0.05	0.05	0.05	0.05

Fig. 17. Heat Loss Data With Shield

DATE	TIME	STD IN	STD OUT	STD DELTA	GRAV FLOW	RHS IN	RHS OUT	RHS DELTA	RHS TPILE	RHS PWR	AIR TEMP	STD OUTPUT	RHS FLOW	DLTA ERR	FLOW ERR	RHS TM-TA	RHS EFF	EFF UNCR	EFF PRBL	RHS LOSS	LOSS POSS	LOSS PRBL
3/20/82	17:16	14.88	22.36	7.48	0.0310	14.99	22.31	7.32	6.73	970.	27.3	977.	1.5	-2.1	1.5	-8.65	100.7	1.7	0.8	XXXX	XXXX	XXXX
3/20/82	17:31	14.21	25.11	10.90	0.0312	14.32	25.12	10.80	9.79	1427.	27.0	1435.	0.4	-0.9	0.4	-7.28	100.5	1.4	0.7	XXXX	XXXX	XXXX
3/20/82	17:54	13.47	27.71	14.24	0.0312	13.59	27.73	14.14	12.86	1878.	26.4	1871.	1.1	-0.7	1.1	-5.74	99.6	1.3	0.6	XXXX	XXXX	XXXX
3/20/82	18:06	17.32	22.84	5.52	0.0627	17.42	22.86	5.44	4.91	1433.	29.7	1461.	-0.4	-1.4	-0.4	-9.56	101.9	1.9	0.8	XXXX	XXXX	XXXX
3/20/82	18:15	16.94	24.11	7.17	0.0626	17.05	24.14	7.09	6.47	1878.	29.3	1892.	-1.1	-1.1	-0.4	-8.70	100.7	1.6	0.7	XXXX	XXXX	XXXX
3/17/82	10:47	29.14	32.88	3.74	0.0312	29.25	32.94	3.69	3.34	489.	29.5	494.	0.4	-1.3	0.4	1.59	100.9	2.6	1.3	XXXX	XXXX	XXXX
3/17/82	11:20	28.85	36.06	7.21	0.0314	28.96	36.12	7.16	6.42	950.	29.2	958.	-0.7	-0.7	-0.1	3.34	100.8	1.7	0.8	XXXX	XXXX	XXXX
3/17/82	11:46	28.60	39.09	10.49	0.0313	28.71	39.19	10.48	9.40	1399.	28.8	1393.	0.1	-0.1	0.6	5.15	99.5	1.4	0.7	XXXX	XXXX	XXXX
3/17/82	12:13	28.64	42.44	13.80	0.0316	28.78	42.53	13.75	12.32	1840.	29.0	1821.	1.4	-0.8	1.4	6.65	99.0	1.8	1.1	XXXX	XXXX	XXXX
3/18/82	13:53	30.50	34.08	3.58	0.0636	30.61	34.09	3.48	3.26	957.	29.1	964.	2.1	-2.8	2.1	3.25	100.8	2.3	1.0	XXXX	XXXX	XXXX
3/18/82	14:13	30.52	35.76	5.24	0.0638	30.60	35.77	5.17	4.77	1413.	28.6	1416.	1.1	-1.3	1.1	4.59	100.2	1.9	0.8	XXXX	XXXX	XXXX
3/18/82	14:33	30.43	37.45	7.02	0.0639	30.55	37.48	6.93	6.34	1880.	27.6	1901.	0.2	-1.3	0.2	6.41	101.1	1.7	0.8	XXXX	XXXX	XXXX
3/18/82	16:18	30.73	31.97	1.24	0.0948	30.78	32.00	1.22	1.16	495.	26.1	498.	1.1	-1.6	1.1	5.29	100.5	4.5	2.1	XXXX	XXXX	XXXX
3/18/82	15:56	30.67	33.11	2.44	0.0954	30.73	33.14	2.41	2.24	972.	26.5	986.	-0.2	-1.2	-0.2	5.43	101.4	2.9	1.3	XXXX	XXXX	XXXX
3/18/82	15:27	30.84	34.40	3.56	0.0948	30.91	34.44	3.53	3.25	1426.	27.8	1429.	0.6	-0.9	0.6	4.88	100.2	2.3	1.0	XXXX	XXXX	XXXX
3/18/82	15:05	30.74	35.39	4.65	0.0951	30.82	35.43	4.61	4.23	1876.	27.5	1873.	1.0	-0.8	1.0	5.62	99.8	2.0	0.9	XXXX	XXXX	XXXX
3/17/82	14:58	58.37	64.93	6.56	0.0328	58.24	65.01	6.77	6.42	946.	28.5	901.	3.2	3.2	1.8	33.13	95.2	1.7	0.8	XXXX	XXXX	XXXX
3/17/82	14:15	57.17	66.68	9.51	0.0336	57.08	66.76	9.68	8.86	1390.	28.9	1337.	1.8	1.8	2.1	33.02	96.2	1.4	0.7	XXXX	XXXX	XXXX
3/17/82	13:51	57.10	69.59	12.49	0.0337	57.01	69.68	12.67	11.73	1820.	29.3	1761.	1.4	1.4	1.9	34.05	96.8	1.3	0.6	XXXX	XXXX	XXXX
3/19/82	11:53	59.27	60.98	1.71	0.0633	59.15	60.95	1.80	1.81	474.	29.1	453.	-0.5	5.3	-0.5	30.95	95.5	3.6	1.7	XXXX	XXXX	XXXX
3/19/82	12:13	59.50	62.85	3.35	0.0635	59.49	62.90	3.41	3.26	927.	29.0	890.	1.8	1.8	2.3	32.19	96.0	2.3	1.0	XXXX	XXXX	XXXX
3/19/82	12:40	59.46	64.50	5.04	0.0634	59.46	64.56	5.10	4.79	1382.	28.9	1337.	1.2	1.2	2.1	33.11	96.8	1.8	0.8	XXXX	XXXX	XXXX
3/19/82	13:04	59.26	65.98	6.72	0.0630	59.25	66.00	6.75	6.30	1821.	29.2	1772.	0.4	0.4	2.3	33.42	97.3	1.6	0.7	XXXX	XXXX	XXXX
3/19/82	13:14	63.41	64.60	1.19	0.0951	63.30	64.59	1.29	1.18	492.	24.4	474.	8.4	-8.4	-4.2	39.54	96.3	4.5	2.1	XXXX	XXXX	XXXX
3/19/82	14:16	59.53	61.82	2.29	0.0948	59.50	61.85	2.35	2.28	936.	29.0	908.	0.952	2.6	0.5	31.67	97.0	2.9	1.3	XXXX	XXXX	XXXX
3/19/82	13:51	59.56	62.92	3.36	0.0947	59.53	62.95	3.42	3.25	1377.	28.7	1331.	0.962	1.8	1.6	32.54	96.7	2.3	1.0	XXXX	XXXX	XXXX
3/15/82	13:33	59.77	64.09	4.32	0.0946	59.75	64.10	4.35	4.14	1762.	29.1	1711.	0.968	0.7	2.3	32.82	97.1	2.0	0.9	XXXX	XXXX	XXXX
3/15/82	15:09	78.11	84.88	6.77	0.0321	77.99	85.02	7.03	6.57	973.	27.8	911.	0.330	3.8	2.9	53.70	93.6	1.7	0.8	XXXX	XXXX	XXXX
3/15/82	14:53	78.25	88.21	9.96	0.0329	78.20	88.30	10.10	9.37	1426.	27.8	1376.	0.336	1.4	2.2	55.45	96.5	1.4	0.7	XXXX	XXXX	XXXX
3/15/82	14:13	78.22	91.00	12.78	0.0329	77.96	91.19	13.23	12.18	1875.	28.3	1767.	0.337	3.5	2.5	56.28	94.3	1.2	0.6	XXXX	XXXX	XXXX
3/16/82	11:06	78.18	81.44	3.26	0.0634	78.10	81.49	3.39	3.22	933.	29.7	867.	0.656	4.0	3.5	50.09	92.9	2.3	1.0	XXXX	XXXX	XXXX
3/16/82	11:27	78.26	83.34	5.08	0.0628	78.25	83.40	5.15	4.87	1394.	29.9	1338.	0.645	1.4	2.7	50.93	96.0	1.8	0.8	XXXX	XXXX	XXXX
3/16/82	11:48	78.48	85.06	6.58	0.0626	78.43	85.09	6.66	6.31	1832.	30.0	1731.	0.655	1.2	4.6	51.76	94.5	1.6	0.7	XXXX	XXXX	XXXX
3/16/82	12:47	78.09	80.30	2.21	0.0945	78.05	80.32	2.27	2.22	939.	29.0	876.	0.986	2.7	4.3	50.18	93.3	2.8	1.2	XXXX	XXXX	XXXX
3/16/82	12:12	78.35	82.73	4.38	0.0954	78.35	82.75	4.40	4.18	1824.	29.4	1753.	0.988	0.5	3.6	51.15	96.1	2.0	0.9	XXXX	XXXX	XXXX
3/20/82	23:19	89.20	96.08	6.88	0.0320	88.94	96.11	7.17	6.52	991.	25.8	927.	0.328	4.2	2.6	66.72	93.5	1.6	0.8	XXXX	XXXX	XXXX
3/20/82	23:34	89.30	99.36	10.06	0.0320	89.03	99.40	10.37	9.52	1437.	25.7	1357.	0.329	3.1	2.7	68.51	94.4	1.4	0.7	XXXX	XXXX	XXXX
3/20/82	23:45	89.36	102.75	13.39	0.0320	89.11	102.78	13.67	12.65	1895.	25.5	1805.	0.329	2.1	2.8	70.44	95.3	1.2	0.6	XXXX	XXXX	XXXX
3/20/82	19:39	89.82	93.18	3.36	0.0629	89.60	93.15	3.55	3.27	964.	24.9	889.	0.646	5.7	2.7	66.47	92.2	2.2	1.0	XXXX	XXXX	XXXX
3/20/82	19:49	89.88	95.02	5.14	0.0625	89.72	95.00	5.28	4.73	1425.	24.8	1352.	0.641	2.7	2.6	67.56	94.8	1.8	0.8	XXXX	XXXX	XXXX
3/20/82	19:59	89.80	96.55	6.75	0.0630	89.62	96.50	6.88	6.13	1876.	24.9	1789.	0.648	1.9	2.9	68.16	95.4	1.6	0.7	XXXX	XXXX	XXXX
3/20/82	20:15	90.40	94.89	4.49	0.0940	90.25	94.89	4.64	4.13	1878.	24.9	1775.	0.962	3.3	2.4	67.67	94.5	1.9	0.9	XXXX	XXXX	XXXX

Fig. 18. Initial Calibration Data

DATE	TIME	STD IN C	STD OUT C	STD DELTA C	GRAV FLOW kg/sec	RHS IN C	RHS OUT C	RHS DELTA C	RHS TPILE DELTA C	RHS PWR W	AIR TEMP C	STD OUTPUT W	RHS FLOW kg/sec	DELTA ERR %	FLOW ERR %	RHS TH-TA C	RHS EFF %	EFF UNCOR POSS	EFF UNCOR PRBL	EFF UNCOR PRBL	RHS LOSS W	RHS LOSS POSS W	RHS LOSS POSS PRBL	RHS LOSS POSS PRBL
5/ 9/82	18:18	11.21	15.03	3.82	0.0628	11.32	15.06	3.74	3.38	980.	25.3	1010.	0.0622	-2.1	-0.9	-12.11	103.0	1.9	0.9	0.9	0.9	0.9	0.9	0.9
5/ 9/82	18:27	11.26	14.98	3.72	0.0629	11.36	15.02	3.66	3.37	977.	25.0	985.	0.0634	-1.6	0.8	-11.81	100.9	1.9	0.9	0.9	0.9	0.9	0.9	0.9
5/ 9/82	18:43	11.12	18.37	7.25	0.0633	11.22	18.37	7.15	6.48	1909.	24.4	1932.	0.0634	-1.4	0.2	-9.60	101.2	1.2	0.5	0.5	0.5	0.5	0.5	0.5
5/ 9/82	18:51	11.29	18.37	7.08	0.0630	11.37	18.41	7.04	6.36	1896.	24.0	1879.	0.0639	-0.6	1.5	-9.11	99.1	1.2	0.5	0.5	0.5	0.5	0.5	0.5
5/ 1/82	15:37	33.92	37.58	3.66	0.0627	33.95	37.61	3.66	3.42	968.	25.2	959.	0.0633	-0.0	0.9	10.58	99.1	1.9	0.8	0.8	0.8	0.8	0.8	0.8
5/ 1/82	15:49	34.06	37.70	3.64	0.0628	34.09	37.75	3.66	3.43	966.	26.6	955.	0.0632	0.5	0.6	9.32	98.9	1.9	0.9	0.9	0.9	0.9	0.9	0.9
5/ 1/82	16: 7	33.87	40.85	6.98	0.0628	33.90	40.92	7.02	6.50	1870.	26.0	1832.	0.0638	0.6	1.5	11.41	97.9	1.2	0.5	0.5	0.5	0.5	0.5	0.5
5/ 1/82	16:31	34.00	40.98	6.98	0.0629	34.02	41.05	7.03	6.51	1878.	24.9	1835.	0.0639	0.7	1.6	12.64	97.7	1.2	0.5	0.5	0.5	0.5	0.5	0.5
5/ 8/82	22:25	49.64	53.28	3.64	0.0638	49.61	53.34	3.73	3.37	983.	24.8	970.	0.0630	2.5	-1.1	26.67	98.7	1.9	0.8	0.8	0.8	0.8	0.8	0.8
5/ 8/82	23: 0	49.75	56.75	7.00	0.0635	49.75	56.80	7.05	6.49	1907.	24.7	1860.	0.0647	0.7	1.8	28.58	97.5	1.2	0.5	0.5	0.5	0.5	0.5	0.5
5/ 8/82	23: 7	49.76	56.69	6.93	0.0638	49.72	56.74	7.02	6.45	1905.	24.6	1849.	0.0649	1.3	1.7	28.63	97.0	1.2	0.5	0.5	0.5	0.5	0.5	0.5
5/ 1/82	18:44	73.53	77.06	3.53	0.0629	73.45	77.06	3.61	3.39	967.	22.9	932.	0.0639	2.3	1.5	52.35	96.3	1.8	0.8	0.8	0.8	0.8	0.8	0.8
5/ 1/82	19: 6	73.34	80.48	7.14	0.0624	73.31	80.48	7.17	6.47	1897.	21.8	1868.	0.0631	0.4	1.1	55.10	98.5	1.2	0.5	0.5	0.5	0.5	0.5	0.5
5/ 9/82	2: 9	90.10	93.70	3.60	0.0622	90.00	93.63	3.63	3.46	981.	22.6	942.	0.0642	0.8	3.2	69.22	96.1	1.8	0.8	0.8	0.8	0.8	0.8	0.8
5/ 9/82	2:26	89.61	96.72	7.11	0.0617	89.55	96.65	7.10	6.68	1912.	22.3	1847.	0.0640	-0.1	3.7	70.80	96.6	1.2	0.5	0.5	0.5	0.5	0.5	0.5
5/ 9/82	2:34	89.19	96.31	7.12	0.0618	89.14	96.24	7.10	6.69	1915.	22.2	1852.	0.0641	-0.3	3.7	70.49	96.7	1.2	0.5	0.5	0.5	0.5	0.5	0.5

Fig. 19. Final Calibration Data

APPENDIX 4

COMPUTER PRINTOUT KEY

TEST FACILITY VERIFICATION

DATE	-	Calendar date of the test
STD TIME	-	Time of the test
REFERENCE HEAT SOURCE:		
INLET TEMP	-	Inlet temperature in °C
OUTLET TEMP	-	Outlet temperature in °C
DELTA TEMP	-	Difference between inlet and outlet temperatures in °C
THERM PILE	-	Temperature rise across core as determined by the thermopile in °C
FLOW RATE	-	Fluid mass flow rate calculated from RHS mea- surements in kilograms per second
INPUT POWER	-	Electrical energy input to core heaters in watts
TEST STAND #:		
INLET TEMP	-	Inlet temperature in °C
OUTLET TEMP	-	Outlet temperature in °C
DELTA TEMP	-	Difference between inlet and outlet temperatures in °C

FLOW RATE	-	Fluid mass flow rate in kg/sec as determined by the test stand flow meter and the calculations necessary to obtain mass flow from volume flow rate
ENERGY GAIN	-	Thermal energy input to the fluid as determined by the test facility instrumentation in watts
AIR TEMP	-	Ambient air temperature during the test in °C
RHS TM-TA	-	Difference between the mean RHS fluid temp and the air temp in °C
DELTA TEMP T/R	-	Ratio of the temperature rise determined by the test stand instrumentation to that determined by the RHS instrumentation
SPFIC HEAT T/R	-	Ratio of the specific heat of the fluid at the mean of the test stand inlet and outlet temperatures to the specific heat at the mean of the RHS inlet and outlet temperatures.
FLOW ERROR	-	Percentage difference between the mass flow rate determined by the test stand instrumentation and the RHS calculations
STAND TM-TA	-	Difference between the mean test stand fluid temperature and the ambient air temperature in °C
ENERGY ERROR	-	Percentage difference between the thermal energy gain measured by the test stand and the electrical energy input by the RHS

		REFERENCE HEAT SOURCE										TEST STAND 1											
DATE	STD TIME	INLET TEMP (C)	OUTLET TEMP (C)	DELTA TEMP (C)	THERM PILE (C)	FLOW RATE KG/SEC	INPUT POWER (W)	INLET TEMP (C)	OUTLET TEMP (C)	DELTA TEMP (C)	FLOW RATE KG/SEC	ENERGY GAIN (W)	AIR TEMP (C)	RHS TM-TA (C)	DELTA TEMP T/R	SPECIFIC HEAT T/R	FLOW ERROR (%)	STAND TM-TA (C)	ENERGY ERROR (%)				
3/3/21/82	15:32	32.79	32.79	0.00	0.02	0.0631	4.	32.76	32.80	0.04	0.0616	10.	28.4	4.4	0.000	1.000	0.0	4.4	0.0				
3/3/21/82	15:57	31.30	34.92	3.62	3.21	0.0629	951.	31.31	34.96	3.65	0.0616	939.	27.1	6.0	1.008	1.000	-2.0	6.0	-1.2				
3/3/21/82	16:12	31.24	34.80	3.56	3.22	0.0645	960.	31.22	34.84	3.62	0.0626	947.	26.9	6.1	1.017	1.000	-3.0	6.1	-1.3				
3/3/21/82	16:17	31.29	34.86	3.57	3.22	0.0642	958.	31.31	34.92	3.61	0.0625	943.	27.0	6.1	1.011	1.000	-2.7	6.1	-1.6				
3/3/21/82	16:27	30.26	37.13	6.87	6.18	0.0643	1845.	30.17	37.06	6.89	0.0626	1802.	27.3	6.4	1.003	1.000	-2.6	6.3	-2.3				
3/3/21/82	16:32	30.35	37.20	6.85	6.17	0.0645	1847.	30.32	37.21	6.89	0.0626	1802.	27.6	6.2	1.006	1.000	-3.0	6.2	-2.4				
3/3/21/82	16:37	30.20	37.10	6.90	6.20	0.0640	1845.	30.29	37.25	6.96	0.0625	1817.	27.5	6.1	1.009	1.000	-2.3	6.3	-1.5				
3/3/21/82	16:55	51.99	51.99	0.00	0.12	0.0631	4.	52.01	51.98	-0.03	0.0623	-8.	27.1	24.9	0.000	1.000	0.0	24.9	0.0				
3/3/21/82	17:12	52.22	55.80	3.58	3.18	0.0631	944.	52.25	55.71	3.46	0.0620	897.	27.0	27.0	0.966	1.000	-1.7	27.0	-5.0				
3/3/21/82	17:17	52.15	55.69	3.54	3.18	0.0641	949.	51.99	55.56	3.57	0.0620	926.	26.8	27.1	1.008	1.000	-3.3	27.0	-2.5				
3/3/21/82	17:22	52.32	55.85	3.53	3.19	0.0639	943.	52.17	55.64	3.47	0.0619	898.	26.8	27.3	0.983	1.000	-3.1	27.1	-4.8				
3/3/21/82	17:27	52.22	59.14	6.92	6.15	0.0634	1835.	52.20	59.00	6.80	0.0619	1760.	26.7	29.0	0.983	1.000	-2.3	28.9	-4.0				
3/3/21/82	17:42	52.02	59.02	7.00	6.46	0.0628	1837.	52.18	59.04	6.86	0.0618	1773.	26.5	29.0	0.980	1.000	-1.5	29.1	-3.5				
3/3/21/82	17:47	52.03	58.92	6.89	6.24	0.0637	1835.	52.05	58.96	6.91	0.0619	1789.	26.3	29.2	1.003	1.000	-2.8	29.2	-2.5				
3/3/21/82	18:27	69.33	69.32	-0.01	0.02	0.0631	4.	69.42	69.27	-0.15	0.0622	-39.	24.7	44.6	0.000	1.000	0.0	44.6	0.0				
3/3/21/82	18:37	69.45	73.10	3.65	3.34	0.0617	944.	69.63	73.15	3.52	0.0617	910.	24.6	46.7	0.964	1.000	-0.1	46.8	-3.6				
3/3/21/82	18:42	69.29	72.87	3.58	3.32	0.0630	945.	69.37	72.88	3.51	0.0616	906.	24.6	46.5	0.980	1.000	-2.2	46.5	-4.2				
3/3/21/82	18:47	69.51	73.09	3.58	3.32	0.0628	942.	69.60	73.10	3.50	0.0617	905.	24.5	46.8	0.978	1.000	-1.8	46.8	-4.0				
3/3/21/82	18:57	69.40	76.31	6.91	6.37	0.0626	1812.	69.58	76.38	6.80	0.0616	1756.	24.5	48.4	0.984	1.000	-1.5	48.5	-3.1				
3/3/21/82	19:12	69.28	76.18	6.90	6.31	0.0627	1812.	69.45	76.24	6.79	0.0615	1750.	24.4	48.3	0.984	1.000	-1.8	48.4	-3.4				
3/3/21/82	19:17	69.47	76.34	6.87	6.33	0.0631	1818.	69.54	76.36	6.82	0.0616	1761.	24.4	48.5	0.993	1.000	-2.4	48.6	-3.1				
3/3/21/82	19:42	93.61	93.55	-0.06	0.02	0.0631	6.	93.85	93.69	-0.16	0.0637	-43.	24.1	69.5	2.667	1.000	0.0	69.7	0.0				
3/3/21/82	19:52	93.52	96.95	3.43	3.12	0.0638	921.	93.79	97.11	3.32	0.0639	893.	24.1	71.1	0.968	1.000	0.2	71.4	-3.0				
3/3/21/82	19:57	93.72	97.13	3.41	3.11	0.0654	940.	93.87	97.19	3.32	0.0640	895.	24.2	71.2	0.974	1.000	-2.2	71.3	-4.8				
3/3/21/82	20:12	93.37	96.81	3.44	3.16	0.0642	929.	93.74	97.07	3.33	0.0640	897.	24.3	70.8	0.968	1.000	-0.2	71.1	-3.4				
3/3/21/82	20:17	93.77	100.30	6.53	5.89	0.0656	1805.	94.07	100.54	6.47	0.0641	1747.	24.2	72.8	0.991	1.000	-2.3	73.1	-3.2				
3/3/21/82	20:22	93.70	100.24	6.54	5.82	0.0645	1777.	94.02	100.56	6.54	0.0640	1763.	24.2	72.8	1.000	1.000	-0.8	73.1	-0.8				
3/3/21/82	20:27	94.05	100.72	6.67	5.80	0.0649	1823.	94.22	100.75	6.53	0.0641	1763.	24.2	73.2	0.979	1.000	-1.2	73.3	-3.3				
3/3/21/82	20:32	93.70	100.84	7.14	6.10	0.0602	1811.	94.05	101.06	7.01	0.0606	1790.	24.1	73.2	0.982	1.000	0.7	73.5	-1.2				

Fig. 20. Facility Verification Data - Sample 1

